DiscThruster Concept—Hyper Efficient Pressure-Thrust Driven Air Breathing and Rocket Propulsion

J. Bradley Pande
iPropulsion, Midway, UT 84049, USA

Historically, propulsion research has focused on maximizing momentum-thrust and minimizing pressure-thrust for optimal engine performance. The DiscThruster™ concept reverses this paradigm by prioritizing pressure-thrust, resulting in conceptual hyper efficient air-breathing and rocket engines. DiscThruster channels low-velocity fluid through a converging-only nozzle, achieving sonic choking at the exit plane that generates pressure-thrust while minimizing momentum-thrust. This approach avoids the large loss of kinetic energy leaving the engine's control volume in the form of high velocity exhaust gases that cannot perform any additional work. For example, a two-phase mixture of liquid bismuth-tin eutectic and gaseous ethanol at 325°C (617°F) chokes at just 17.6 m/s (57.7 ft/s) at a pressure of 40 bar (580 psi). The high-density eutectic in a two-phase mixture promotes very low sonic velocities for effective fluid capture and recycling. This concept focuses on producing a 129 kN (29,000 lbf) thrust class DiscThruster engine for commercial narrow body aircraft, powered by a small conventional air breathing turboshaft engine. The rocket engine version uses the same DiscThruster core but substitutes the small turboshaft engine with an electric motor and battery combination to power the space launch vehicle to orbit. Sized at < 1.0 m (< 3.3 ft) in diameter, DiscThruster's disc is relatively compact to produce required thrust. Experimental hardware testing with air-water mixtures at room temperature and pressures up to 6.9 MPa (1,000 psi) validated the concept's ability to empirically create and measure two-phase flow sonic choking in a rocket nozzle and demonstrate fluid exiting the nozzle can be captured and recycled using centripetal force by means of high 5,300 rpm spinning blades. DiscThruster's closed-form analysis predicts hyper efficient pressure-thrust airbreathing and rocket propulsion concepts exceed their goals of reducing fuel burn by 50% when benchmarked against modern high bypass turbofan engines, and a 2X or doubling in specific impulse over high performance liquid rocket engines. Since predicted DiscThruster performance exceeded goals, a knock down factor (added margin for uncertainty) was included to match goals.

I. Nomenclature

ρ_g = density of gas kg/m^3 (lbm/in^3)
A_e = area at nozzle exit plane m^2 (ft^2)
α_g = volume fraction of gas (unitless)
α_l = volume fraction of liquid (unitless)
BPR = bypass ratio (unitless)
C = speed of sound of mixture m/s (ft/s)
CFD = computational fluid dynamics
C_l = speed of sound of liquid m/s (ft/s)
C_g = speed of sound of gas m/s (ft/s)
HEM = homogeneous equilibrium model
Isp = Specific impulse N·s/kg (lbf-s/lbm)
KE = kinetic energy J (ft-lbf)
m = mass kg (lbm)
$\dot{m}$ = mass flow rate kg/s (lbm/s)
$MEMS$ = micro-electro-mechanical systems
ρ_l = density of liquid kg/m^3 (lbm/in^3)
ρ_{mix} = density of gas and liquid mixture kg/m^3 (lbm/in^3)
P_e = pressure of gases just upstream of nozzle exit plane Pa (psi)
P_∞ = pressure (usually atm.) downstream of nozzle exit plane Pa (psi)
PLA = polylactic acid, a plastic used in 3-D printing
$PDMS$ = Polydimethylsiloxane, a silicone oil
rpm = revolutions per minute
$TSFC$ = thrust specific fuel consumption (g/(kN·s) (lbm/(lbf·hr))
S = slip ratio (unitless)
shp = shaft horsepower
$SSTO$ = single stage to orbit
T = thrust N (lbf)
UDF = unducted fan
V_e = velocity of exhaust at the exit plane m/s (ft/s)
3-D = three dimensional
η = Mechanical efficiency (unitless or expressed as a percentage)

II. Introduction

Since the introduction of the "rocket equation" shown in Equation 1, scientists have focused on maximizing momentum-thrust, the first term, and minimizing pressure-thrust, the second term, to achieve high specific impulse (Isp) rocket performance. Ideally, the pressure-thrust term is eliminated by expanding gases in the diverging section of a de Laval rocket nozzle until the exit pressure matches ambient external pressure, resulting in the "perfectly expanded" condition. According to current scientific consensus, this condition yields the highest possible propulsive efficiency.

$$\mathrm{T} = \dot{\mathrm{m}}\, V_e + A_e\,(P_e - P_\infty) \qquad \text{Eqn. (1)}$$

The challenge in significantly boosting rocket motor Isp and improving turbofan engine thrust specific fuel consumption (TSFC) lies in reducing the substantial, unrecoverable kinetic energy loss at the control-volume boundary. This loss appears as high-velocity exhaust gases leaving the control volume without performing additional useful work.

By way of hypothetical example, Figure 1 illustrates a converging-diverging de Laval rocket nozzle where expanding gases leave the nozzle at 1,700 m/s (5,577 ft/s) with a mass flow rate of 1.179 kg/s (2.60 lbm/s). The nozzle expansion ratio (not shown to scale in this illustrative example) is set to under-expand the gases in a 90:10 split between momentum-thrust and pressure-thrust at 2,002 N (450 lbf) and 222 N (50 lbf), respectively, for a total thrust of 2,222 N (500 lbf). From the classical kinetic energy (KE) Equation 2, we observe that the velocity-squared term increases kinetic energy non-linearly.

$$\mathrm{KE} = \frac{\mathbf{1}}{\mathbf{2}}\,\mathrm{m}\,{V_e}^2 \qquad \text{Eqn. (2)}$$

This example produces kinetic energy per second or power *leaving* the control volume equal to 1.7 MW (2,285 hp), performing no additional useful work. This underperforming solid rocket motor, with an Isp of 192 seconds (well below industry standards), is limited in part by nozzle under-expansion that produces measurable pressure-thrust. Pressure-thrust that contributes 10% to overall rocket thrust.

For the case of turbofan engines, the approach is to minimize the velocity of accelerated air leaving the engine and the lost kinetic energy it carries with it. Today designers aim for increasingly higher fan bypass ratios (BPR). BPR is the ratio of air mass bypassing the engine core through the outer fan to the air mass passing through the engine core. The strategy is to accelerate *larger* masses of air at *lower* velocity changes, thereby imparting less kinetic energy to the air exiting the engine's control volume. However, practical limits exist. As turbofan engine cowls grow in diameter, internal and external drag diminish performance gains. Consequently, engine manufacturers are revisiting Pratt & Whitney/Allison's unducted fan (UDF) technology from the 1980s, which achieved very high BPRs using highly swept, counter-rotating propeller blades—without the drag penalties associated with large turbofan ducting and external shrouds. This may represent the *practical limit* of turbofan/turboshaft fuel burn reductions, offering only marginal gains over current modern systems.

Figure 2 illustrates a single rocket nozzle of DiscThruster's pressure-thrust-based propulsion device. DiscThruster may consist of a hundred or more of these small rocket nozzles that collectively generate the required thrust. In this example, 200 small DiscThruster nozzles, each producing 11.1 N (2.5 lbf) of thrust, when combined equal 2,222 N (500 lbf), matching the solid rocket motor thrust shown in Figure 1. For this comparison, we ignore momentum-thrust by setting it to zero (bring all fluid to rest) and assume receiver pressure is zero (vacuum). The working fluid travels down the converging only nozzle and sonically "chokes" at the exit plane. The two-phase fluid consists of liquid bismuth-tin eutectic and gaseous ethanol at 325°C (617°F) and 40 bar (580 psi), with a 97.5:2.5 liquid-to-gas volumetric ratio, choking at just 17.6 m/s (57.7 ft/s) based on Equation 3.

Actual *static* pressure at the choke point would be set higher to account for receiver pressure and pressure drop in the nozzle. Two-phase fluid exiting all 200 nozzles, with a density of 7,020 kg/m³ (438 lbm/ft³), carries a kinetic energy per second of only 10.6 kW (14.2 hp). For the DiscThruster concept to be technically successful, the following conditions must be met:

(1) Working fluid exiting the nozzles must be virtually 100% recaptured, reconditioned, and recycled back to the nozzles—this is the largest challenge the previous experimental hardware sought to demonstrate.

(2) Working fluid passing through the exit plane requires a "clear view of the sky," allowing downstream pressure to equal or near equal ambient atmospheric pressure (P_∞).

(3) Performance estimates shall have > 25% performance margin *above* the goals of a 50% minimum reduction in turbofan fuel burn and a 2X doubling of Isp over liquid rocket engines, as built in margin for uncertainty.

(4) Two-phase fluids must not be toxic to humans or the environment based on Environmental Protection Agency or equivalent international regulatory hazard codes.

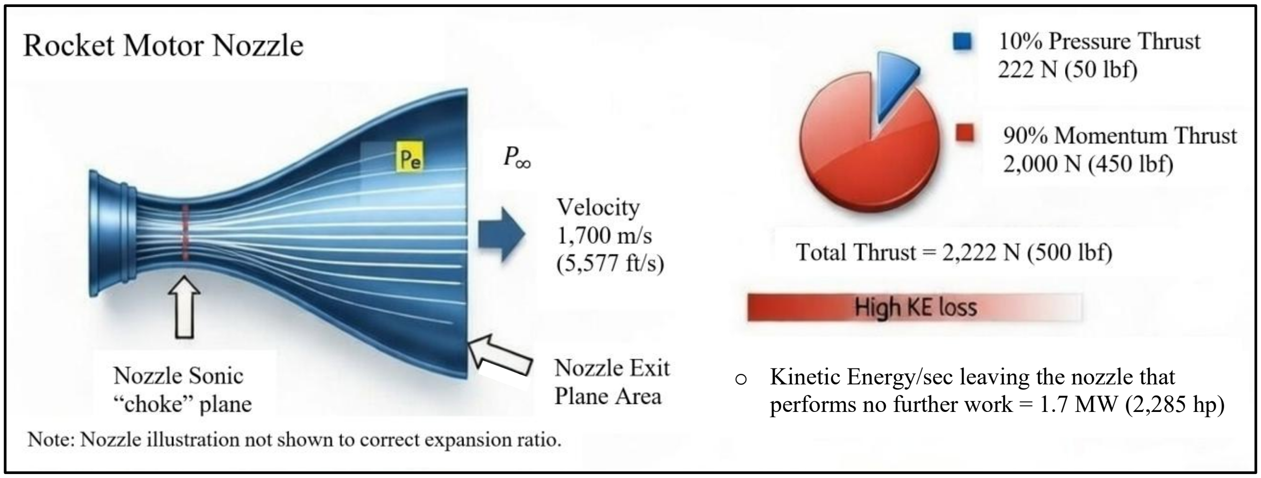

- Kinetic Energy/sec leaving the nozzle that performs no further work = 1.7 MW (2,285 hp)

Figure 1. Rocket motor total thrust derived from both momentum and pressure-thrust. Large kinetic energy losses in the form of high-velocity gases leave the nozzle at a rate of 1.7 MW (2,285 hp).

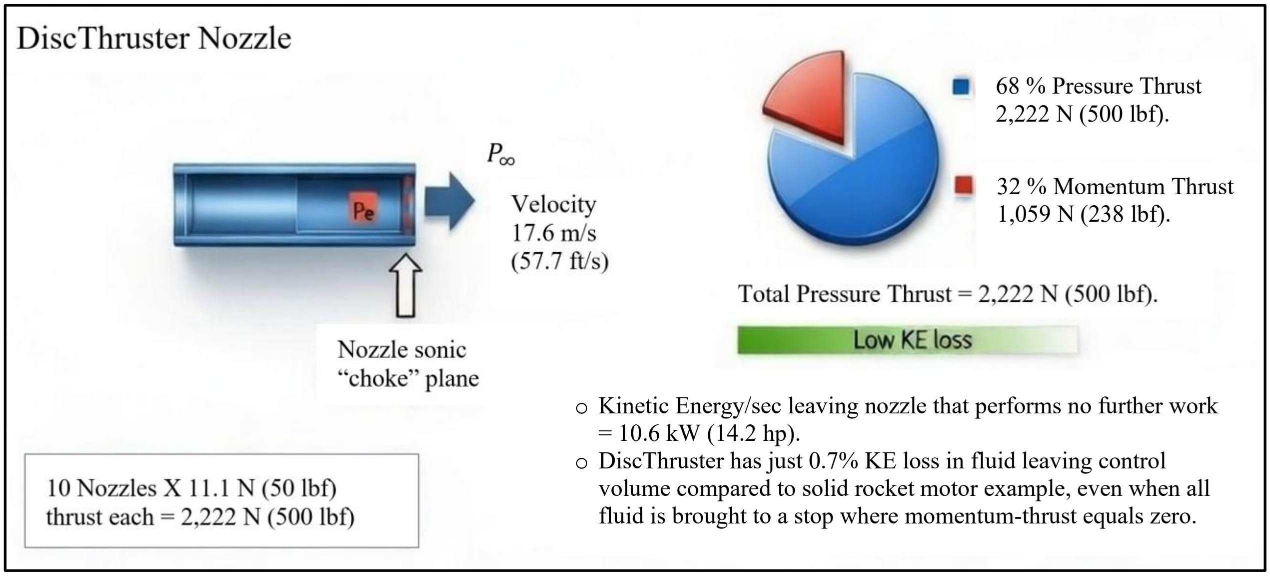

- Kinetic Energy/sec leaving nozzle that performs no further work = 10.6 kW (14.2 hp).
- DiscThruster has just 0.7% KE loss in fluid leaving control volume compared to solid rocket motor example, even when all fluid is brought to a stop where momentum-thrust equals zero.

Figure 2. DiscThruster “chokes” two-phase fluid at just 17.6 m/s (57.7 ft/s) compared to the rocket motor’s 1,700 m/s (5,577 ft/s), reducing non-recoverable KE to just 0.7% of the rocket motor—the primary driver to DiscThruster’s potential hyper gains in performance.

Table 1 summarizes Figures 1 and 2 overall results for a hypothetical the 2,222 N (500 lbf) thrust device. As illustrated previously, the DiscThruster concept is grounded in the *rocket equation* and does not depend on any other concept to operate.

DiscThruster and Solid Rocket Motor Comparison

Thruster Configuration	Total Thrust N (lbf)	Momentum Thrust[1] [MT] (%)	Pressure Thrust (%)	Exhaust Velocity m/s (ft/s)	Power (KE/s) Loss in Exiting Exhaust kW (hp)	Discussion
Solid Rocket Motor (SRM)	2,222 (500)	90	10	1,700 m/s (5,577 ft/s)	1,700 kW (2,285 hp)	Large KE losses leave system doing no additional work.
DiscThruster	2,222 (500) MT set to zero[1]	32 → 0 MT set to zero	68	17.6 m/s (57.7 ft/s)	10.6 kW (14.2 hp)	DiscThruster has only 0.7% KE loss compared to SRM for same thrust.

Notes:
1. For this DiscThruster example, all fluid exiting nozzle is brought to zero velocity before being recycled back to system. Recovered kinetic energy (KE) is zero—worst case. DiscThruster experiments demonstrated successful KE fluid recovery using an impulse turbine similarly used in hydroelectric power generation plants.

Table 1. DiscThruster's small 0.7% kinetic energy loss points to the opportunity for hyper performance gains when compared to solid rocket motors.

III. Procedure

A. Analytical Approach to Calculating Two-phase Sonic Velocities and Candidate Down-Select

DiscThruster concept performance is tied to the use of low sonic-velocity fluids flowing through rocket nozzles. Two-phase fluids consist of a homogeneous mixture of liquid and gas and typically exhibit sonic velocities that are orders of magnitude lower than those of either constituent alone. For example, air and water have sonic velocities of 331 m/s (1,086 ft/s) and 1,403 m/s (4,600 ft/s), respectively. However, when combined into a two-phase fluid with a 50:50 liquid-to-gas volumetric mixture, the sonic velocity calculated using Wood's equation (Eq. 3) is only 60.5 m/s (198.5 ft/s) at 22.4 bar (325 psi) pressure. Lower operating pressures produce lower sonic velocities.

It is noteworthy that one researcher has predicted that "in a water–steam mixture the sound speed [sonic velocity] may be as low as ~1 m/s under equilibrium conditions along the saturation curve" (Ref. 1). This suggests that the development of "engineered ultra-low, or hyper-low," sonic-velocity fluids could represent a key enabling technology for the DiscThruster concept.

Woods closed-form equation (see Eq. 3 and Table 2) has been used accurately for decades to predict two-phase sonic velocities and remains well-validated in the literature. Numerous variations and refinements of the original Wood's equation have been proposed. For the present application, the same formulation is applied across both high and low liquid volumetric fractions by adjusting the slip ratio, as described below.

(1) *High Volumetric Liquids* (liquid fraction ≥ 50 %) with isothermal bubbly/liquid-dominated flow mixtures the Slip-augmented Homogenous Equilibrium Model (HEM) used was S = 1.25.

(2) *High Volumetric Gases* (liquid fraction < 50 %) with gas volume dominated mixtures including light mists S=1.0 was used.

Wood's is a closed-form equation and may not accurately predict sonic velocity under all two-phase flow conditions. Nevertheless, it serves as an effective trade-study and sensitivity-analysis tool that provides a foundation for future Computational Fluid Dynamics (CFD) analyses, which are beyond the scope of the present study. It is important to note that some commercial CFD solvers are more capable than others when modeling two-phase sonic choking. Therefore, careful solver selection is critical for accurate results.

As two-phase fluids accelerate while entering the converging section of a nozzle (Bernoulli effect), the lower-density gas phase tends to accelerate more rapidly than the higher-density liquid phase, primarily due to inertial and thermal effects. Upon reaching the minimum-area choking plane, the gas phase may be traveling at a higher velocity than the liquid phase, which results in increased effective sonic velocity.

The method that accounts for this phenomenon is called slip ratio. Slip ratio (S) is defined as the velocity of the gas phase divided by the liquid phase velocity exiting the nozzle. When S equals 1.0 the gas and liquid phases travel the same speed through the nozzle. In two-phase flows the slip ratio is influenced not only by density differences between the liquid and gas phases, but also by wall friction, boundary layer development, turbulence, and viscous effects.

There are many academic sources calculating slip ratios differently, resulting in a wide range of sonic velocity values, some of which predict higher sonic velocity values than what we are using in our study. Based on our engineering assumptions we chose a slip ratio of 1.25 for high liquid volumetric fractions (>50% liquid), and a slip ratio of S=1.0 for high gas volumetric fractions (< 50% liquid). Should slip ratio effects prove significant during future experimental testing, design approaches exist to impart additional velocity to the liquid phase, or lower velocities to the gas phase prior to reaching the choking plane. Thereby ensuring that both phases reach the choking condition at near equal velocities ($S \approx 1.0$). Risks related to potentially high slip ratios are included in Table 5's Risk Assessment and Mitigation Matrix, part of the highest recorded risk on the chart.

$$C = \left[\rho_{mix}\left(\frac{\alpha_g}{S\rho_g^2} + \frac{\alpha_l}{\rho_l^2}\right)\right]^{-0.5} \quad \text{Eqn. (3) Ref. (2)}$$

Equation 3. Woods equation predicts sonic velocities for two-phase fluids.

A wide range of two-phase fluid combinations were evaluated with the objective of achieving the lowest possible sonic velocity at a minimum operating temperature of 260 °C (500 °F), while prioritizing environmentally responsible constituents. High-temperature two-phase working fluids enable the DiscThruster concept to employ more compact, and lighter-weight heat exchangers, since the temperature differential between the high-and-low temperature reservoirs governs heat extraction performance. Although not an absolute requirement, the practical upper operating temperature of the DiscThruster may be constrained employing titanium Ti-6Al-4V for high-temperature structural components, given its maximum continuous operating temperature is approximately 500 °C (932 °F).

The trade study summarized in Table 2 identified several promising candidates that satisfy the combined requirements of low sonic velocity, elevated operating temperature, and environmentally acceptable liquid and gas constituents. A broad range of working fluids were evaluated, including single-phase and multiphase systems (some incorporating a solid third phase), spanning cryogenic temperatures through titanium service temperatures and beyond. In addition, several theoretical working fluids with idealized properties were assessed. Table 2 represents a selected subset of potential candidates and does not necessarily reflect the author's preferred choices. Because sonic velocity in two-phase fluids varies significantly with liquid-to-gas volumetric mixture ratio, sonic velocities for each candidate fluid are reported at multiple mixture ratios.

Most available legacy data focuses on water–air and steam–water systems, including behavior along their saturation lines. Many research efforts in conventional and nuclear power generation rely on steam as their working fluid. Similarly, natural-gas pipeline operators are highly concerned with high-velocity gas transport, when inadvertent sonic choking occurs at pinch points from only a few percent of moisture entrainment accumulating in the pipeline, dramatically reducing flow rates. In both applications, sonic choking represents a critical operational limitation to be avoided, not exploited.

Propylene glycol and air mixtures are included in Table 2 due to their potential for low sonic velocity, moderate operating temperatures, and environmentally benign characteristics. Propylene glycol is commonly used in aircraft de-icing operations and as a food additive in ice cream. Silicone oils, such as polydimethylsiloxane (PDMS), were also evaluated because of their low bulk modulus, which theoretically promotes reduced sonic velocity. In addition, n-Octane was considered as it transitions to the gas phase at moderate to high temperatures and contributes to low sonic velocity. While silicone oils present environmental and practical concerns, such as slippery surfaces in the event of leaks on runways or tarmacs, n-Octane is relatively environmentally benign, though it is combustible in the presence of oxygen. n-Octane is a widely produced industrial chemical, distilled by the petrochemical industry in a manner like gasoline and diesel fuel, and available at moderate cost.

Table 2 identifies a bismuth tin eutectic alloy (58 wt.% Bi, 42 wt.% Sn) combined with ethanol as the baseline two-phase working fluid for this study. Bismuth tin is solid at room temperature, with a eutectic melting point of 138 °C (280 °F), which is significantly lower than the melting points of either constituent metal alone. The lowest predicted sonic velocities occur at very high liquid volumetric fractions, corresponding to molten metal with a small fraction of evenly distributed entrained gas. A volumetric mixture of 97.5% liquid and 2.5% gas, highlighted in blue in Table 2, was selected as the baseline condition with a calculated sonic velocity of 17.6 m/s (57.7 ft/s). Although a lower gas content of 1% yields a modest reduction in sonic velocity, the 2.5% gas fraction provides a practical safety margin to avoid inadvertent transition to a fully liquid (single phase) condition, where sonic velocity would increase by orders of magnitude. From an operational perspective, a lower gas fraction may ultimately be preferable, as the system strategy emphasizes gas recovery and condensation within a compact heat exchanger rather than reliance on a more power intensive multi-stage axial gas compressor currently in the baseline.

Sonic Choke Velocities for Select Two-phase Fluids

Two-Phase Liquid/Gas	Volumetric liquid:gas Ratio (unitless)	Temp and Pressure ºC (ºF) [bar (psi)]	Choke Velocity m/s (ft/s)	Slip Ratio	Comments
Water/Air	50:50 75:25 95:5 5:95	21 (70) [22.4 (325)]	60.5 (198.5) 69.9 (229.3) 138.7 (455.0) 51.9 (170.3)	1.25 1.25 1.25 1.00	Water-Air combination has largest empirical data base. Some isothermal two-phase steam-gas combinations predict choking as low as 1 m/s (3.3 ft/s) at low pressure. See Ref. 1.
Propylene Glycol/ air	50:50 75:25 95:5 5:95	121 (350) [22.4 (325)]	57.1 (187.3) 68.8 (225.7) 136.2 (446.9) 87.2 (386.1)	1.25 1.25 1.25 1.00	Thermal heat up in system requires heat exchanger to dissipate heat away. Propylene Glycol has higher operating temperature and low toxicity. Sonic velocity is high.
PDMS Silicone Oil/ air	50:50 75:25 95:5 5:95	200 (392) [22.4 (325)]	137.6 (451.4) 159.2 (522.3) 315.8 (1036.1) 92.4 (303.1)	1.25 1.25 1.25 1.00	Silicone fluids have low bulk modulus and higher operating temperatures. Potentially low velocity choking but calculations show it is high.
Bismuth Tin/ n-Octane	99:1 97.5:2.5 50:50 5:95	288 (550) [22.4 (325)]	16.3 (53.5) 17.6 (57.7) 26.2 (86.0) 58.7 (192.6)	1.25 1.25 1.25 1.00	Runner-up to Bismuth Tin eutectic and ethanol gas . Chokes at same velocity but can't operate at as high pressure as ethanol.
BASELINE Bismuth Tin/ Ethanol	99:1 **97.5:2.5** 50:50 5:95	**325 (617)** [40.0 (580)]	16.3 (53.5) **17.6 (57.7)** 26.4 (86.6) 58.2 (191.0)	1.25 **1.25** 1.25 1.00	DiscThruster's baseline design; two-phase fluid of Bismuth Tin eutectic and ethanol gas at a 97.5:2.5 mix ratio (only 2.5% gas by volume in mixture).

Table 2. Sonic velocities were calculated for select two-phase fluids. Bismuth-tin eutectic and ethanol were selected as the baseline.

B. Summary of DiscThruster Hardware Testing and Follow on Concepts

Table 3 summarizes five distinct DiscThruster hardware test apparatuses and conceptual design configurations. Each design is described in detail in subsequent sections (C through G), as indicated in the "Paper Section" column. Collectively, the table provides an evolutionary snapshot of the DiscThruster architecture, illustrating how the core design has progressed based on experimental results and lessons learned from preceding configurations.

The selection of bismuth tin as the liquid constituent in a two-phase working fluid may initially appear counterintuitive. This high-density material must first be heated to a molten state before ethanol vapor can be introduced. However, at the molecular scale, a homogeneous and isothermal mixture consisting of very dense liquid atoms surrounded by a sparse gas phase (2.5% by volume) exhibits fundamentally different acoustic behavior. In such a mixture, large impulse-momentum forces are required to accelerate the liquid molecules via pressure (sonic) waves propagating between the gas and liquid phases. This interaction results in significantly reduced effective sonic velocity.

Summary of DiscThruster Hardware Testing and Follow-on Concepts

Paper Section	Descriptive Title	Illustration	Purpose	Results
C Fig. 3	Stationary Nozzle Thruster on Inverted Pendulum Thrust Stand		• Build thrust stand with converging only rocket nozzle and measure thrust for two-phase water/air fluids at different volume fractions and pressures.	• Momentum-thrust and pressure-thrust successfully measured over wide range including pressures up to 6.9 MPa (1,000 psia). Recorded sonic velocities.
D Fig. 5	First Generation Spinning Disc with No Fluid Recapture		• Build and test 3D printed spinning DiscThruster disc. Pass fluid between three rows of 48 nozzles each and exit fluid at right angles to the rotation axis while producing no thrust.	• Successfully built and tested disc spinning at 5,300 rpm. Right angle directed fluid produced no thrust as planned. Demonstrated fluid recapture potential.
E Fig. 14	Second Generation Spinning Disc with Fluid Recapture/ Recycling	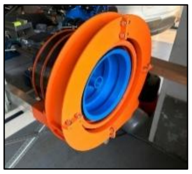	• Build and test spinning DiscThruster disc (blue). Pass fluid between rows of nozzles and exit fluid through a water turbine (not shown) to recapture KE, then collect fluid in volute (orange) to recycle back.	• Successfully demonstrated fluid capture and extraction of KE using the water turbine for zero thrust. Volute (orange) design was undersized and became overwhelmed with mass flow. Needs redesign and internal impeller to move fluid along.
F Fig. 15	First Generation Stationary Disc with Rotating Sweeper Blades to Collect Fluid	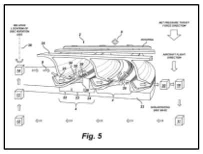	• Concept only (Ref. 4). No hardware built. • Fluid exiting *stationary* concentric rings of nozzles is captured by rotating sweeper blades that redirect fluid back to the next outer row of nozzles, where fluid passes through them. When fluid reaches disc outside diameter, it's recycled back to the first concentric ring of nozzles.	
G	First Generation Reciprocating-Pulsing Disc with Rotating Sweeper Blades to Collect Fluid	Concept only.	• In design stage. No hardware built. • Reciprocating/pulsing disc moves back-and-forth along the nozzle centerline, forcing stationary fluid to choke in the nozzle, exiting the nozzle with near zero velocity. The rotating sweeper blades collect and recycle fluid back to the nozzles. Approach provides half the thrust (needs twice area) of rotating Disc but minimizes fluid KE momentum losses. May also be configured into thin flat panels.	

Table 3. Summary of DiscThruster hardware testing and follow-on concepts.

A material selection requirements matrix was applied and bismuth tin and ethanol produced some of the lowest calculated sonic velocities at elevated operating temperatures, while meeting environmental considerations, with the understanding that ethanol has an autoignition temperature near its operating temperature of 363 °C (685 °F) in the presence of air.

A DiscThruster baseline operating condition of 40.0 bar (580 psi) and 325 °C (617 °F) was selected, as this point lies within ethanol's gaseous phase and remains below and to the right of its critical point on the ethanol phase diagram. Increasing the pressure beyond ethanol's critical pressure of 61.4 bar (891 psi) would transition the working fluid into a supercritical state, in which it would likely no longer exhibit the low-sonic-velocity behavior characteristic of a two-phase gas–liquid mixture. While numerous gaseous candidates with higher critical pressures could serve as substitutes for ethanol, a deliberately conservative baseline configuration was selected for this study.

In general, higher operating pressures enable a more compact DiscThruster design that can improve overall system efficiency, due in part to reduced circulating working-fluid and their kinetic energy losses associated with lower frictional effects.

C. DiscThruster - Stationary Single Nozzle Water-Air Two-Phase Flow Testing

To understand behavior of two-phase fluid sonically choking in a converging only nozzle, an inverted pendulum thrust stand was constructed as shown Figure 3 illustration. An inverted thrust stand has a pivot axis (A) at its base of the test stand and an arm extending vertically up. Mounted atop the arm is the rocket nozzle (I). Adjacent to the arm is the *stationary* thrust-stand tower (B), to which a force meter (C) is attached but not visible in the current view. The 0–111 N (0–25 lbf) dial-type force meter is zeroed when the rocket nozzle is not producing thrust and measures thrust magnitude when two-phase fluid flows through the nozzle. A brief history of the inverted-pendulum thrust stand is provided below as follows:

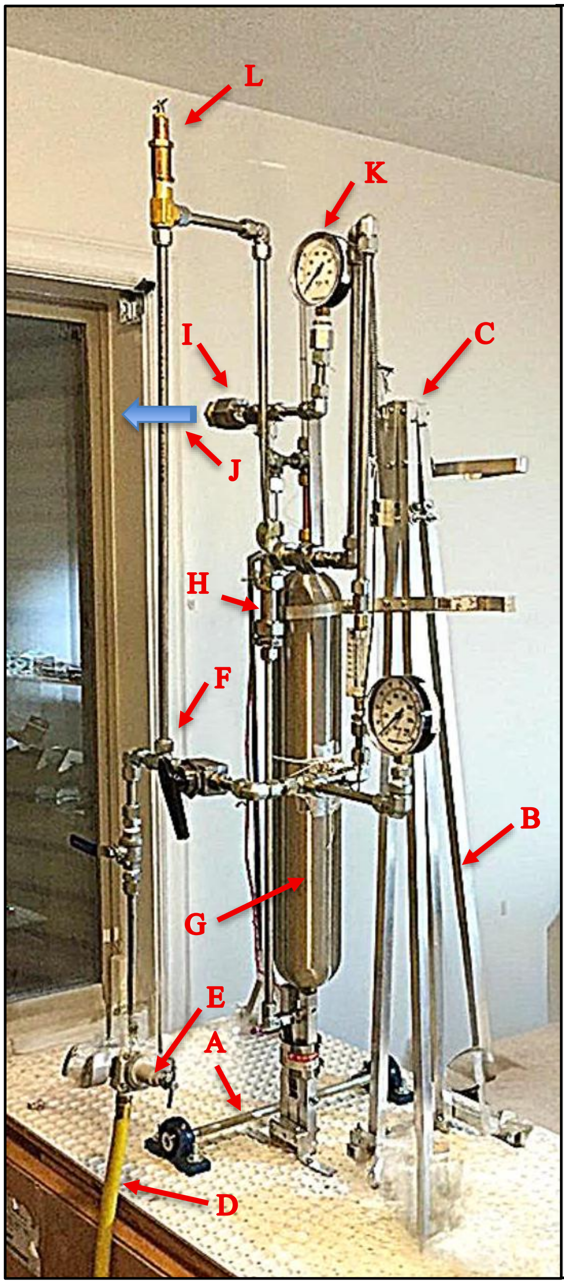

<u>Inverted Pendulum Thrust Stand Description</u>

A—Inverted pendulum thrust stand pivot axis (axle).
B—Inverted pendulum thrust stand stationary tower reacts against nozzle thrust without moving.
C— Force meter (blocked in this view). Measures rocket nozzle thrust as inverted pendulum pushes against stationary tower (B).
D—Main pressure line into thrust stand.
E—Main pressure line pressure regulator.
F—Main pressure line splitter. Pressurizes fluid reservoir in sample cylinder (long silver cylinder) and supplies gas to two-phase fluid atomizer.
G—Sample cylinder reservoir filled with distilled water.
H—Two-phase fluid atomizer. Water and gas are mixed prior to entering rocket nozzle.
I—Rocket nozzle with interchangeable diameters.
J—Two-phase fluid leaving rocket nozzle exit plane.
K—Pressure gage reading static nozzle back pressure.
L—Pressure relief safety valve. Installed for high temperature saturated steam testing that was later abandoned due to safety concerns.

<u>Operation</u>

Rocket thruster pivots on an inverted pendulum axis (A) [pendulum shown dismounted from the axle]. Thrust generated by the rocket pushes against the stationary tower (B) and is measured by a dial type force meter (C) [blocked in picture]. High pressure regulated air (D) is split at a "T" pipe section (F) where some gas is plumbed to the top of the double ended silver sample cylinder (G), pressurizing water contained in it. The other split side injects gas into the two-phase atomizer (H) where air and water mix, creating two-phase fluid prior to entering the rocket nozzle. This is a pressure-blowdown system where the water reservoir usually empties before the gas reservoir becomes unable to maintain set regulator pressure.

Figure 3. Pressure blow-down test stand where two-phase fluid (water and air) chokes inside a converging rocket nozzle and thrust is recorded.

1) Test Apparatus - An inverted-pendulum thrust stand developed to test water–air two-phase flows at room temperature using a single, interchangeable converging only rocket nozzle. Preliminary experiments with high-temperature saturated water were attempted but ultimately deemed too hazardous for both the test hardware and operating personnel. Testing was conducted in a blow-down configuration as previously discussed.

2) Purpose of Test - The objective of the test campaign was to generate two-phase flow and accurately measure rocket-nozzle thrust over a wide range of pressures and volumetric mixture ratios using a single nozzle throat diameter ranging from 3.175 to 9.525 mm (0.125 to 0.375 in). For high-pressure tests, smaller nozzle diameters were employed to ensure at least five seconds of steady measurable thrust. This approach prevented depletion of the 3.785-liter (one gallon) sample-cylinder reservoir (labeled G in Fig. 3) and avoided pressure decay below the regulator set point. For maximum pressure runs, the pressure regulator was removed, and flow was supplied directly from a scuba tank in a true blow-down configuration. A representative result from these tests is shown in Figure 4. During blow-down operation transition from sonic to subsonic flow regimes was both audible and visually observable.

3) Conclusions - Static testing with interchangeable converging nozzles was largely successful. Two-phase flow was reliably generated in the two-phase fluid atomizer (labeled H), introduced into a converging-only nozzle, and produced measurable momentum-thrust. Pressure-thrust was then back calculated. After careful balancing, the inverted-pendulum thrust stand demonstrated stable and repeatable performance. Reasonable agreement was observed between closed-form calculations (Table 2) and experimental results at different water–air volumetric ratios with reduced correlation at higher or lower water fractions.

4) Lessons Learned – Accurate determination of two-phase mass flow rate for the test stand shown proved challenging. Additionally, it was predicted and observed that as the ratio of ambient pressure to throat pressure approached approximately 0.53, flow became increasingly unstable, being on the cusp of minimum pressure ratio to sustain sonic choking. Although the hardware was designed to allow heating to generate saturated steam, early testing indicated that such operation posed unacceptable safety risks and was not pursued.

5) Reflections - The inverted-pendulum static thrust stand provided valuable experience and confidence in working with low-velocity room-temperature two-phase flows and converging nozzle designs. Converging only nozzles were intentionally used to avoid further fluid acceleration to minimize the momentum-thrust component. These results supported proceeding to the next development phase that focused on capturing and recycling the working fluid downstream of the rocket nozzle.

D. DiscThruster Spinning Disc – Open Loop Fluid (Not Recycled)

After gaining an understanding of two-phase flow behavior in a stationary, sonic-choking rocket nozzle of previous Section C, sufficient confidence was established to proceed with development of a rotating DiscThruster incorporating a series of non-sonic-choking nozzles, as shown in Figs. 5 and 6. In this configuration fluid passes through successive stages of nozzles driven by centripetal forces generated by disc rotation. These forces both repressurize the flow prior to entry into subsequent rocket nozzles, and then captures and direct the total flow toward circumferential exit passages at the outer rim of the disc.

In this design, the working fluid exits the control volume, operating in an open-loop configuration. An open-loop system does not attempt to recover or recycle the working fluid after it leaves the DiscThruster. In contrast, the closed-loop approach described in the following section D attempts to capture and recycle all working fluid back to the nozzle inlets, such that no fluid exits the system. The DiscThruster rotor shown in Figs. 5 and 6 was fabricated using 3-D additive manufacturing from polylactic acid (PLA) thermoplastic and has an overall diameter of 24 cm (9.5 in).

The DiscThruster shown in Figs. 5 and 6 consists of four concentric circumferential rings, each containing a series of small rocket nozzles. Each ring contains 48 rocket nozzles, for a total of 192 nozzles. Fluid is introduced only at the innermost ring of nozzles. When the DiscThruster is spun up to 5,300 rpm, fluid exiting these inner-ring nozzles possesses both a vertical velocity component and a significant tangential velocity component. Adjacent radial fins, or "scoops," collect the tangentially outward-moving fluid while increasing its pressure through centripetal acceleration before it enters the next larger circumferential ring of nozzles. This process repeats through successive nozzle rings until the fluid reaches the outer circumferential exit slots, where it discharges completely from the disc, thereby operating as an open-loop system.

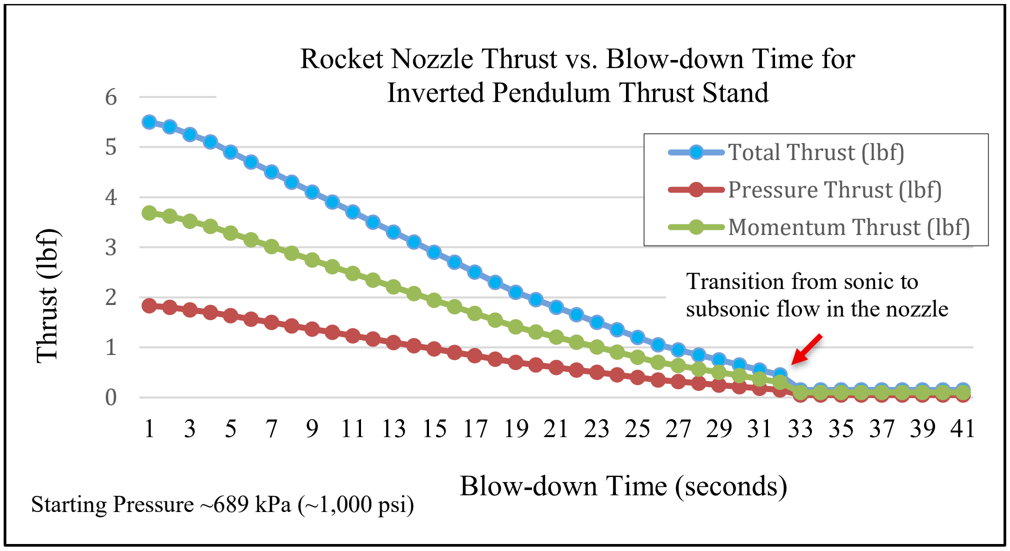

Figure. 4 Thrust stand blow-down test results at starting pressure of ~689 kPa (~1,000 psi). Two-phase fluid flowing through nozzle transitions from sonic to subsonic at 32 seconds as observed by sudden thrust drop on the curve.

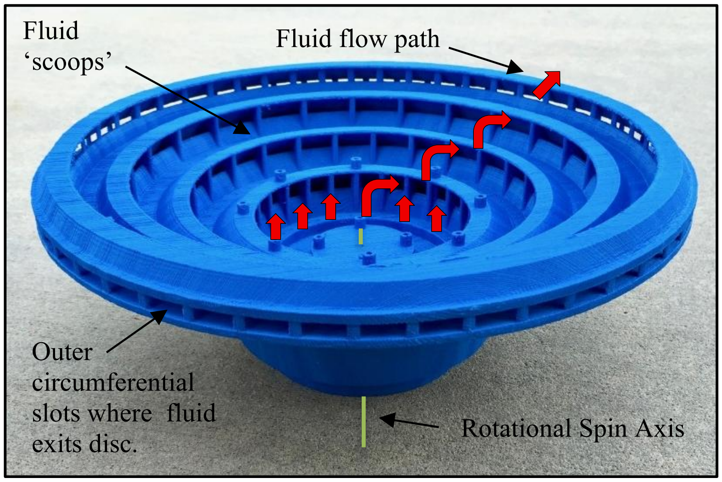

Figure 5. DiscThruster fluid flow path shown as red arrows travels from the inner ring of rocket nozzles, passes through three additional rings of nozzles, and exits out the edge of the disc.

Figure 6. DiscThruster plan view shows four circumferential rows of rocket nozzles.

Figure 7 illustrates the DiscThruster in operation. As the disc rotates, it redirects the non-two-phase working fluid through a 90-deg change in flow direction. In the leftmost image, water exits the nozzles of the stationary non-rotating disc. As the disc spin accelerates, shown in the center image, centripetal forces progressively "bend" the nozzle flow through a right-angle turn. In the rightmost image, the disc is operating at full rotational speed, and fluid exits uniformly around the disc perimeter in a nearly planar "sheet." Under this condition, the net thrust is effectively zero, as intended by the design.

Figure 8 shows the complete DiscThruster experimental setup mounted on the thrust stand. Major components include two engines, the largest one to rotate the disc and smaller one to pump fluid into the disc through a hollow rotating shaft. Also included are the drive chain that couples the large engine to the DiscThruster, bearing assemblies, and thrust-measurement hardware.

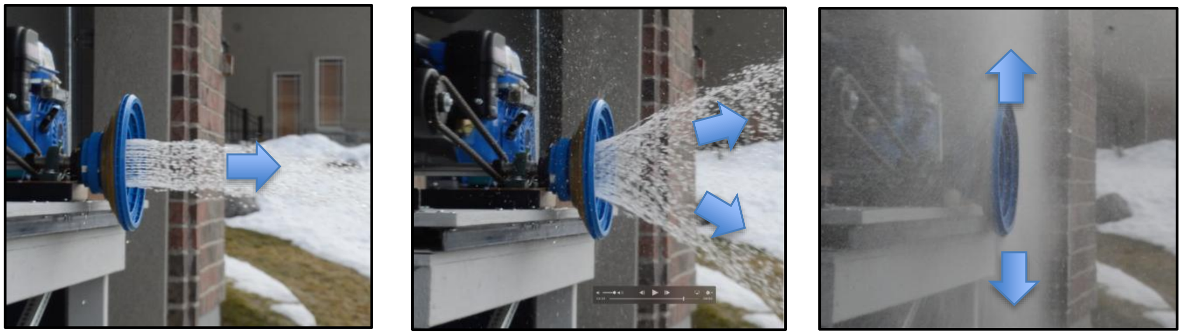

Figure 7. Spin up sequence for DiscThruster where all the fluid exits out the perimeter while producing zero thrust as planned.

E. DiscThruster Rotating Open-Loop (Fluid Not Recycled) - Purpose, Design, and Test Highlights

DiscThruster rotating open-loop operation and results are as follows:

(1) DiscThruster Operation - The DiscThruster consists of four concentric circumferential rings, each containing 48 small rocket nozzles, for a total of 192 nozzles. Working fluid supplied through a rotating hollow axle shaft feeds the innermost nozzle ring. As the fluid exits the nozzles, it travels outward with a dominant tangential velocity component that intersects and impinges on a series of flat radial fins, or "scoops," located between each nozzle ring. These fins capture, redirect and repressurize the flow before it enters a subsequent nozzle ring. After exiting the outermost nozzle ring, the fluid is discharged through circumferential passages at the disc perimeter, operating as an open-loop system. The disc is driven by a large gasoline engine coupled with the disc shaft via a chain drive. A second, smaller engine pumps water into the system, while a gas reservoir injects air into the water stream to simulate two-phase flow. The entire apparatus is mounted on a thrust stand that directly measures rocket nozzle thrust.

(2) Purpose of the Test - The purpose of this test was to route working fluid through the spinning disc's inner nozzle ring, successively recapture and redirect the flow through three additional nozzle rings, and ultimately expel fluid out the disc's outer circumference while producing zero net thrust.

(1) Test Results - After multiple trials and design refinements, fluid was successfully redirected ("bent") through all rocket nozzle rings and discharged circumferentially from the disc perimeter. Throughout testing, the thrust stand registered essentially zero net thrust, thereby achieving the primary design objective.

(2) Conclusions - The DiscThruster open-loop rotating-disc design was largely successful and served as an effective pathfinder for subsequent DiscThruster design iterations. The primary objective, producing zero net thrust while redirecting the working fluid through a 90-deg change in direction relative to the nozzle centerlines—was achieved. These results validated the fundamental operating concept and supported progression to future advanced DiscThruster configurations.

(3) Lessons Learned - The radially flat "scoop" geometry, while effective in transferring fluid between successive nozzle rings proved to be hydraulically inefficient, effectively "slapping" the fluid into the next nozzle stage. Future designs will replaced this geometry with a hydraulically efficient curved scoop profile that reduce losses and improve flow guidance.

Structural reinforcement of the spinning disc presented several challenges. Wrapping the disc with Kevlar® composite to carry hoop stresses induced by high rotational speeds was difficult to implement. Future designs will replace Kevlar with carbon-fiber composite overwraps, a material that is easier to handle and integrate structurally. This design did not allow fiber hoop overwrap reinforcement placement over the delicate circumferential edge slots that were fabricated from low-strength PLA plastic. As a result, these unsupported edge features fractured under high rpm centripetal loading. Future designs will incorporate continuous carbon-fiber composite reinforcement at the disc circumference edge to avoid this structural limitation.

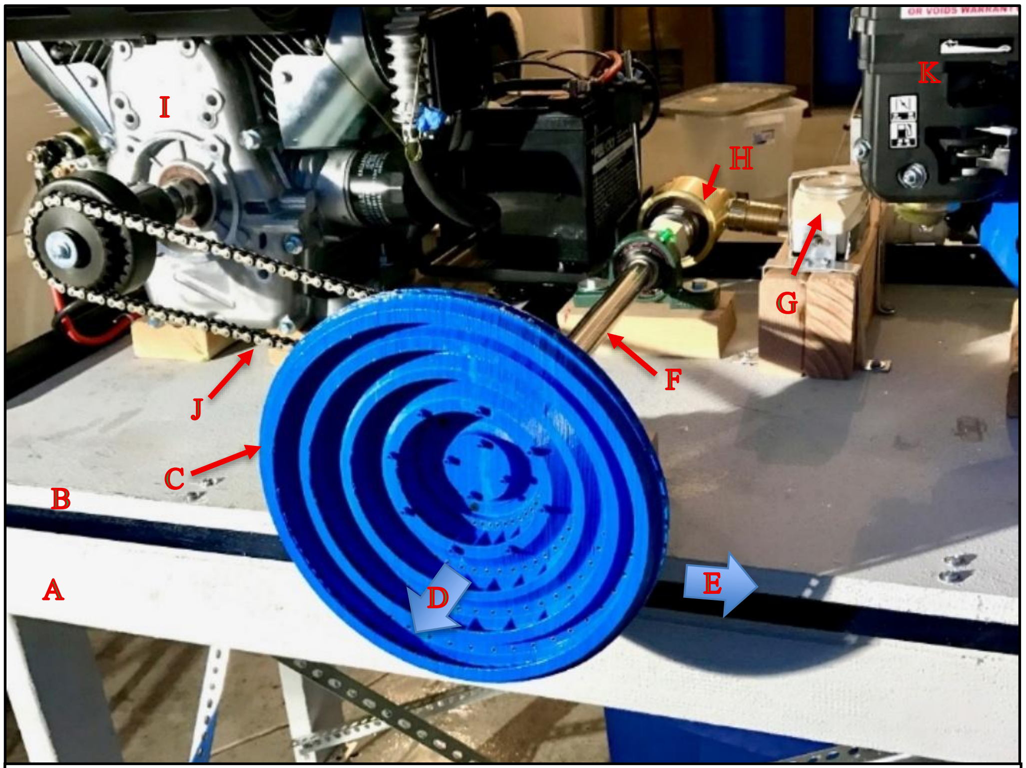

Component Description:

A. Thrust stand base. Stationary part fixed to ground.

B. Thrust stand. Moving part where the platform slides on linear bearings parallel to the DiscThruster's centerline and axle (F).

C. DiscThruster disc.

D. DiscThruster disc rocket nozzle fluid flow direction when not spinning. Parallel to axle.

E. DiscThruster disc fluid flow path when spinning. Flow “bends 90º into a plane at right angles to the axle.

F. DiscThruster drive shaft. Hollow shaft center flows liquid only or liquid and gas in a non-two-phase air-water mixture through its center.

G. Dial type force meter. Connected between the stationary test stand base (A) and the sliding linear ball bearing thrust stand top (B). Measures DiscThruster thrust.

H. Rotating joint. Couples rotating axle to stationary mount allowing fluid to pass through hollow axle.

I. 16.4 kw (22 hp) commercial gasoline engine with attached dry clutch.

J. Chain drive delivering engine power to the DiscThruster drive shaft (F).

K. Gasoline engine powered water pump that feeds pressurized water to hollow shaft.

L. Large capacity water container reservoir rests on the ground (not shown).

M. Gas pressure reservoir air supply tank attached to commercial electric driven air compressor to fill it. Gas is introduced into the hollow drive shaft through a pressure regulator to control flow rate to simulate air entrainment to produce non-two-phase flow. All components rest on the ground (all not shown).

Figure 9. DiscThruster on thrust stand with major components labeled.

Figure 10. DiscThruster's closed cycle design exhibits two sets of nozzle rings and a composite structural overwrap.

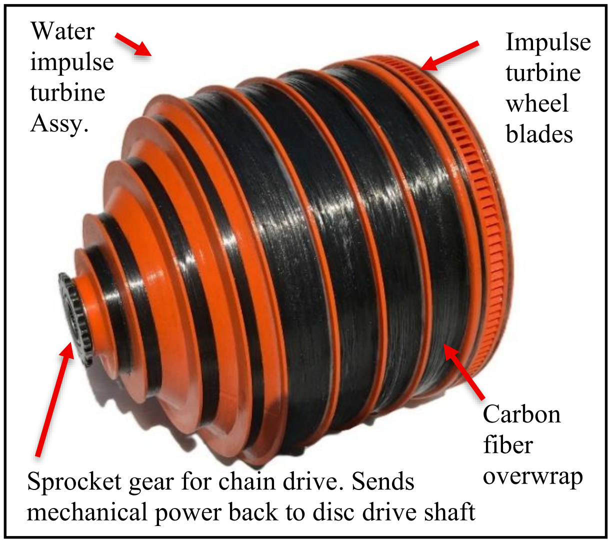

Figure 11. Geared water impulse turbine is made from 3-D printed thermoplastic and overwrapped with carbon fiber composites.

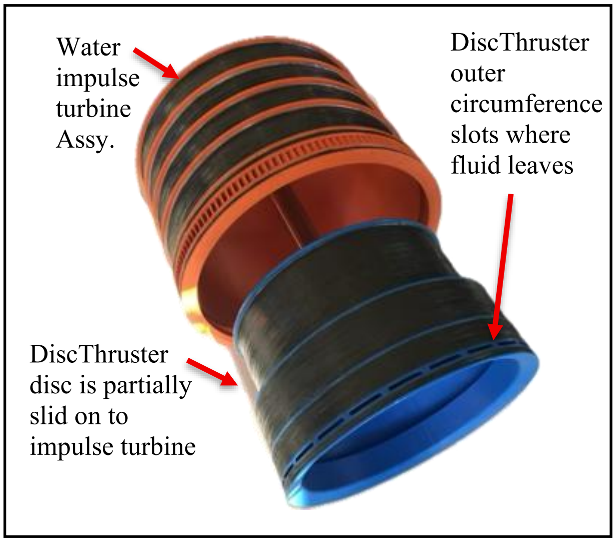

Figure 12. Geared water impulse turbine slips over the DiscThruster disc and aligns to the impulse turbine wheel.

As predicted from analysis, only very small amounts (< 1%) of entrained air can be tolerated in the working fluid entering the DiscThruster because the rotating disc incorporates an integral ‘centrifugal’ or otherwise centripetal water pump to self-pressurize the fluid prior to reaching the first nozzle ring. Entrained air disrupts this mechanism and stalls internal pumping action and pressurization. Consequently, future DiscThruster designs that employ two-phase working fluids will require separation of the liquid and gas phases until immediately upstream of the rocket nozzles. Furthermore, due to density differences between liquid and gas phases in the nozzle itself, high centripetal accelerations rapidly separate two-phase mixtures, increasing effective sonic velocity or eliminating the ability to achieve sonic choking altogether. This behavior limits rotating disc configurations primarily to saturated liquids, supercritical fluids, or other working fluids with nearly uniform density components. Limited two-phase operation may be possible under low rotational acceleration conditions, but this constraint must be carefully managed in future designs.

F. DiscThruster - Water-Air Flowing Through a Spinning Disc in Closed Loop System (Fluid Recycled)

Many components from the previous open-loop test stand were repurposed for the closed-loop DiscThruster configuration, including both commercial gasoline engines used to drive the rotating disc and pump water into the system. Several upgrades were implemented for this phase of testing. These included a new metal base plate for the thrust stand, replacement of the mechanical dial force meter with a digital force meter, and the addition of a larger pressurized gas reservoir to pre-pressurize the working fluid prior to entry into the hollow drive shaft and disc. Flow-measurement capability was also improved by adding of a digital water flow meter and a conventional rotameter (variable area flow meter) for gas flow, enabling more accurate control of two-phase volumetric mixture ratios entering the hollow axle.

The new DiscThruster disc represents a simplified evolution of the previous open-loop design, incorporating several improvements derived from lessons learned. Key changes included a redesigned scoop geometry, replacement of the Kevlar overwrap with a Hexcel IM7® carbon fiber composite overwrap cured with room-temperature epoxy resin, reduction to two nozzle rings, and numerous other refinements. The design focused on the following objectives:

(1) Reduction of Fluid Flight Time - Minimize fluid “flight time” to less than 2 milliseconds, measured from the moment the fluid exits the nozzle plane to when it reaches the radially outer scoop vanes, after traveling along a predominantly tangential trajectory.

(2) Kinetic energy recovery via impulse turbine - Incorporate a geared water impulse turbine to capture kinetic energy from the fluid exiting the spinning disc’s outer circumference and mechanically return energy to the drive shaft through a gear and chain transmission.

(3) Closed-Loop Fluid Recovery - Incorporate a volute, a toroidal (doughnut-like) cavity that collects fluid leaving the impulse turbine and returns it to the water reservoir for continuous recycling.

(4) Simulated Two-Phase Flow - Simulate two-phase flow conditions through the rocket nozzles, recognizing that true two-phase flow could not be sustained under high rotational acceleration due to centripetal force separation of the gas and liquid phases within the nozzle.

Figure 10 on the previous page shows the closed-loop DiscThruster mounted on its drive shaft. While based on the same operating principles as the open-loop configuration, this version incorporates multiple design improvements. Notably, the external carbon-fiber composite overwrap provides structural reinforcement to the outer circumference, preventing failure at high rotational speeds, a limitation observed in earlier designs.

Figures 11 and 12 on the previous page show the orange water impulse turbine that slides over the DiscThruster disc and rotates independently of the drive shaft. The turbine is supported by roller bearings fixed to the outer diameter of the drive shaft, allowing it to rotate freely at a different speed, typically a little less than half the disc rotational speed. This configuration enables the impulse turbine to extract kinetic energy from the tangentially exiting fluid and transmit it back to the drive shaft via the sprocket (shown in Fig. 10) and drive chain (not shown), while still allowing excess fluid velocity to exit the turbine.

The DiscThruster impulse turbine operates on the same fundamental principle employed by large hydroelectric power plants, where fluid kinetic energy is converted into electrical power.

Figure 13 presents a partially disassembled view of the closed-loop DiscThruster. The rotating disc (blue) directs high-velocity, tangential flow toward the inner diameter of the impulse turbine wheel (orange). The turbine blades redirect the flow through an approximate 160-170° angle turn, capturing most of the fluid’s kinetic energy. Residual fluid velocity then enters the volute, where it is guided along the outer walls and exits through a bottom hole. Recovered kinetic energy is mechanically transferred back to the DiscThruster’s hollow drive shaft via a multi-sprocket and chain transmission.

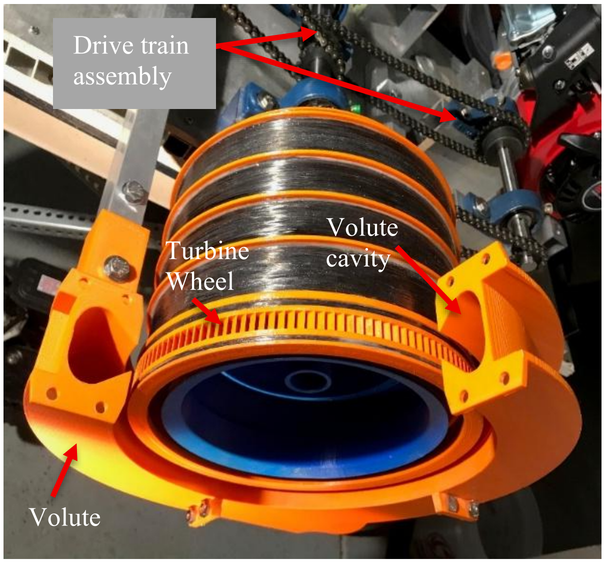

Figure 13. Partially disassembled volute is designed to capture water exiting the impulse turbine.

Figure 14. Fully assembled DiscThruster including disc, impulse turbine wheel, and volute.

Figures 14 and 15 show the fully assembled closed-loop DiscThruster mounted on the thrust stand. This configuration is designed to capture and recycle working fluid exiting the rocket nozzles, enabling fully closed-cycle operation. Key details are summarized below.

(1) Test Apparatus - The DiscThruster consists of a 24 cm (9.5 in) diameter disc fabricated by 3-D additive manufacturing from polylactic acid (PLA) thermoplastic. The disc and impulse-turbine wheel assembly are structurally reinforced with a Hexcel IM7® carbon-fiber composite overwrap cured in a room-temperature epoxy matrix to withstand high rotational hoop stresses. The DiscThruster disc (blue) incorporates two concentric circumferential nozzle rings, each containing 48 individual rocket nozzles.

The fluid-transfer "scoops" feature a swept, curved geometry, representing a significant improvement over the flat radial fins used in earlier designs. These scoops capture fluid exiting the inner nozzle ring and redirect and pressurize it efficiently into the subsequent larger-diameter nozzle ring. After passing through all nozzle stages, the fluid exits the disc at the circumferential edge and enters the impulse turbine wheel, operating as a closed-loop system in which no fluid leaves the test-apparatus control volume.

High-velocity tangential flow passes through the impulse turbine, where most of its kinetic energy is extracted in in the form of reduced velocity. The fluid then enters the surrounding circumferential volute (orange), which collects the flow and directs it downward under gravity back to the water reservoir. The recovered fluid is subsequently recycled back to the DiscThruster via the hollow drive shaft.

(2) Purpose of the Test - The purpose of this test was to demonstrate closed-loop fluid capture and recycling in a spinning DiscThruster configuration, such that no working fluid exits the device (goal) and the thrust stand registers zero net thrust. No attempt was made to generate two-phase choking thrust while the disc was rotating at high speed.

(3) Test Results - After multiple test iterations and design refinements, the system successfully redirected ("bent") the flow exiting the rocket nozzles, conveyed it through all nozzle rings, discharged it out the disc perimeter to the impulse turbine, and captured most of the fluid within the volute. Throughout testing, the thrust stand consistently registered essentially zero thrust, thereby achieving the primary test objective.

The closed-loop DiscThruster design performed as intended, demonstrating that fluid exiting the rocket nozzles can be effectively captured and recycled back to the system. The redesigned swept-geometry scoops significantly improved fluid transfer between nozzle ring stages, and the impulse turbine successfully captured and reduced fluid exit velocity while recovering a portion of the flow's kinetic energy. Additionally, replacing the Kevlar composite overwrap with carbon fiber tow material proved straightforward and resulted in a more practical and robust structural design solution.

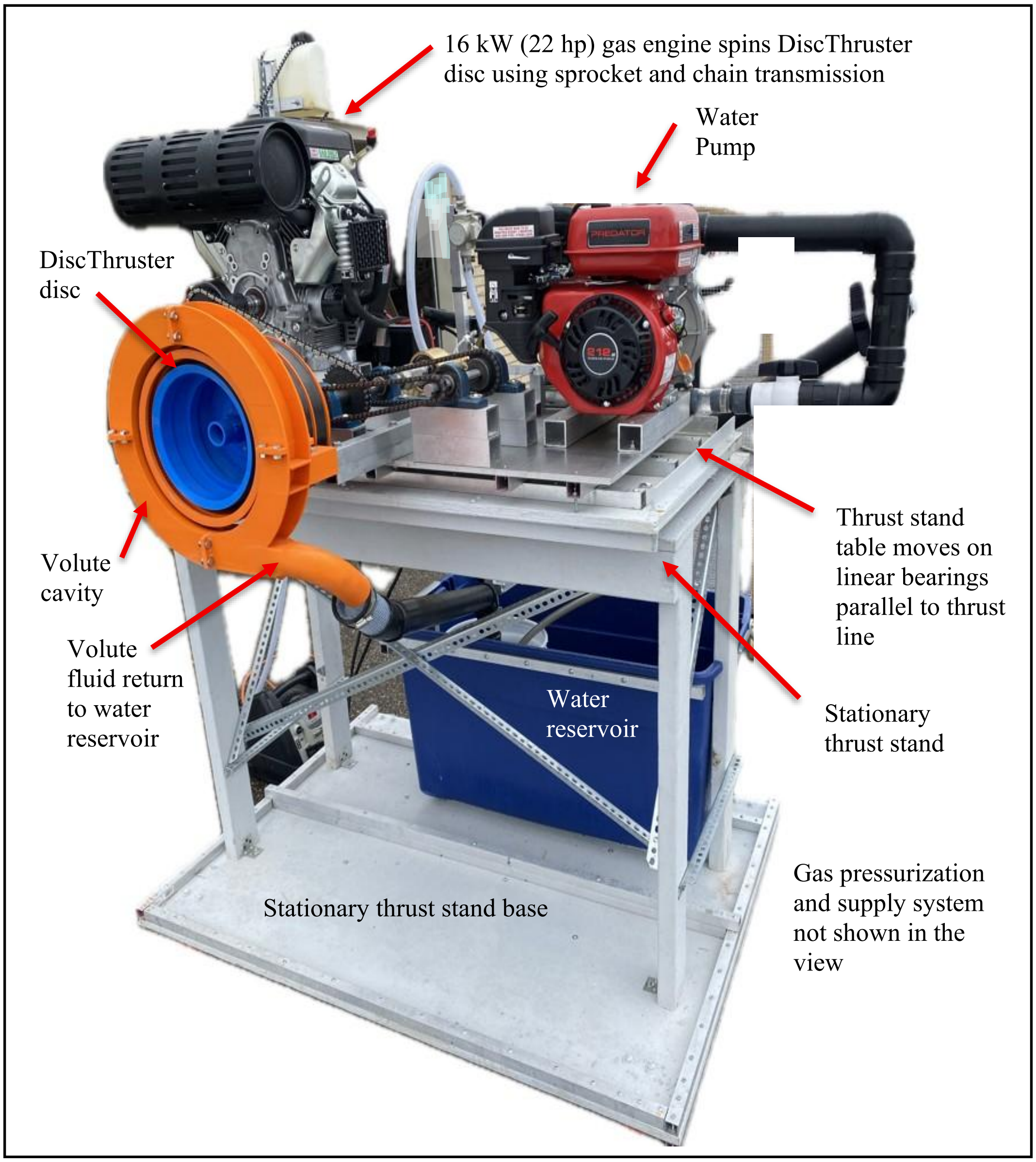

Figure. 15 DiscThruster with closed loop fluid recycling mounted on its thrust stand.

There were challenges encountered during testing. One issue involved the roller-bearing assembly that allowed the impulse turbine to rotate freely on the DiscThruster drive shaft. In the initial configuration, a single roller-bearing sleeve was installed over and rigidly attached to the hollow drive shaft. The outer diameter of this sleeve was then attached to the impulse-turbine wheel, permitting the wheel to rotate independent of the drive shaft, regardless of whether the shaft itself was rotating. During initial spin-up tests the impulse-turbine wheel exhibited excessive vibration due to an insufficient roller-bearing "track width" length. This issue was resolved by adding a second roller-bearing sleeve, which provided additional support and eliminated the vibration.

Another challenge was insufficient fluid throughput within the volute. The approximately 7.6 cm (3 in) diameter exit opening at the bottom of the volute was undersized, causing fluid to back up within the volute cavity. Future designs require an improved volute configuration, potentially incorporating small internal rotating blades or other flow-assistance features to increase fluid evacuation and prevent over accumulation.

G. DiscThruster Stationary Disc with Fluid Capture and Recycling via Rotating “Sweeper” Blades

Figure 15 is an excerpt from the author’s earlier DiscThruster patent application and illustrates a configuration featuring a stationary disc base (33) with fixed rocket nozzles (29). In this concept a set of rotating “sweeper” blades (35) operates at high rotational speed to intercept the working fluid as it exits the stationary rocket nozzles. The sweeper blades capture the flow and redirect it radially outward toward successive circumferential rings of nozzles, traveling from left to right in Figure 15. The working fluid ultimately reaches the outer circumferential edge of the disc where an impulse turbine (not shown) extracts kinetic energy from the high-velocity tangential flow, thereby reducing fluid exit velocity. Recovered kinetic energy is then transmitted mechanically back to the rotating sweeper blades to assist in driving their rotational motion.

Following energy extraction liquid and gas phases are separated. The gaseous component is either routed through a heat exchanger and condensed back into a liquid phase or directed into an axial vane compressor. The liquid and gas are later reconditioned and recombined into a two-phase working fluid. The reconstituted working fluid is then returned to the DiscThruster rocket nozzles, enabling fully closed-loop operation.

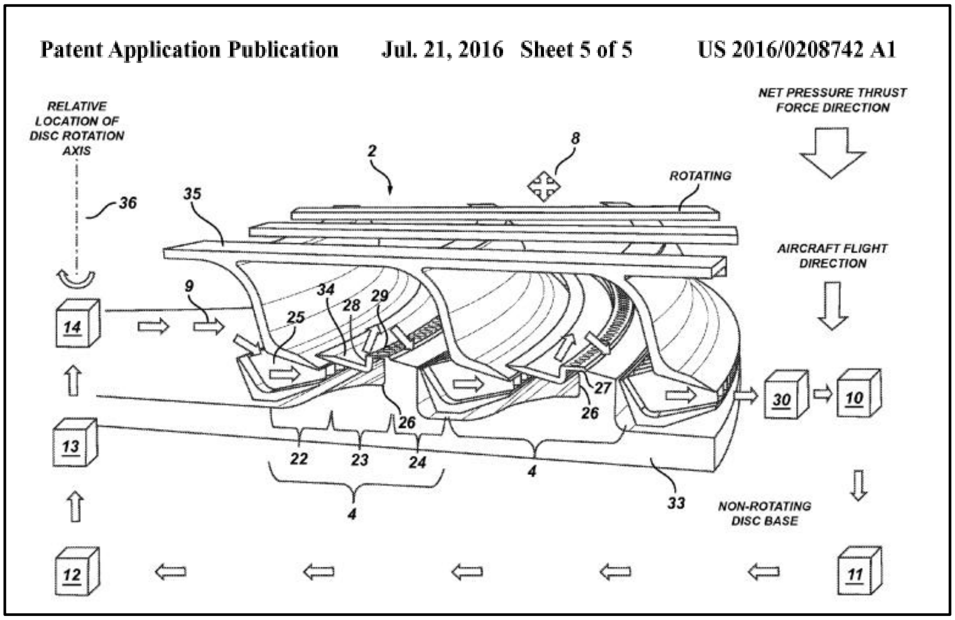

Figure. 15 DiscThruster patent application excerpt shows a stationary disc with rotating blades that capture and recycle fluid leaving the rocket nozzles.

H. Reciprocating-Pulsing Disc with Rotating Sweeper Blades for Closed Loop Collection

The reciprocating-pulsing DiscThruster concept employs rotating “sweeper” blades to collect and recycle working fluid in a closed-loop configuration. This design represents a new conceptual approach while no hardware has been constructed to date.

In DiscThruster operation most of the mechanical power required to produce thrust is expended in forcing the two-phase working fluid through a converging-only rocket nozzle, where power scales as the product of force and velocity. In non-reciprocating DiscThruster configuration, substantial power is required to repeatedly accelerate and decelerate the two-phase liquid as it passes through the nozzle. This effect becomes particularly significant when the liquid phase consists of a high-density material such as a bismuth tin eutectic, which has a specific gravity approximately 7.2 times that of water. In such cases, the kinetic energy required to accelerate and deaccelerate the dense liquid can significantly degrade overall system performance.

One method to reduce this kinetic-energy penalty is to operate the DiscThruster at higher pressures, thereby reducing the total working-fluid volume and thereby its mass. An alternative and complementary approach is to minimize acceleration of the fluid itself. In the reciprocating-pulsing DiscThruster concept, the two-phase working fluid remains relatively stationary, while the rocket nozzle reciprocates (moves) up and down along the nozzle's centerline, forcing the fluid through the nozzle.

During the downward stroke of the reciprocating motion the rocket nozzle moves at or moderately above the sonic choking velocity of the working fluid, creating pressure-thrust. Ideally, the fluid remains near stationary as it is expelled through the nozzle, after which rotating sweeper blades collect the discharged fluid and return it to the system for recycling. This approach requires approximately twice the nozzle thrusting area compared to a non-reciprocating DiscThruster configurations but potentially reduces kinetic-energy losses associated with bulk fluid acceleration. The gaseous component of the two-phase working fluid is collected downstream and recompressed prior to recombination with the liquid phase. To mitigate vibration induced by pulsed operation, multiple reciprocating-pulsing devices would be coordinated within a single disc or square, analogous to the phase-offset operation of pistons moving in cylinders in an automotive engine.

Both the rotating-disc and reciprocating-pulsing DiscThruster concepts can be configured as thin, modular panels integrated into the exterior aerosurfaces of aircraft or space-launch vehicles. Each panel may contain arrays of miniature thruster devices, potentially extending down to micro-electro-mechanical systems (MEMS) scale. MEMS-based thrusting panels could be fabricated using thick silicon wafer etching techniques, as demonstrated in the microelectronics industry. While individual devices produce relatively low thrust per unit area, the use of large surface areas enables the aggregate thrust to meet system-level requirements. These devices like other configurations could operate at high temperatures, where heat dissipation through black body radiating surfaces would be employed, eliminating the need to carry cooling fluids.

I. DiscThruster Major Component Layout and Mechanical Efficiency Calculation

Figure 16 shows DiscThruster's major component layout and mechanical efficiency (η) estimates for each component. Equation 4 defines mechanical efficiency expressed as a percentage.

$$\eta = \frac{Mechanical\ Power\ out}{Mechanical\ Power\ in} \text{ x } 100\% \quad \text{Eqn. 4}$$

Equation 5 calculates DiscThruster's turboshaft power output requirement using the product of force times velocity of the two-phase fluid passing through the converging only rocket nozzles divided by the mechanical efficiency (η) of the system. An additional "performance knockdown factor," is not included in this equation that decrements DiscThruster's engineering estimate performance to match the stated goals of this paper.

$$\text{Power} = \frac{T\ x\ V_e}{\eta} \quad \text{Eqn. 5}$$

Figure 16 displays major components of the closed-loop DiscThruster Sect. G design with just a single concentric row of nozzles, and their labeled component descriptions. Mechanical-efficiency estimates are summarized in Table 5.

A. Turboshaft Engine - The turboshaft engine provides shaft horsepower required to drive the DiscThruster system. It's sized to overcome all mechanical and hydromechanical losses while producing 129 kN (29,000 lbf) of thrust. In addition to propulsion requirements, the turboshaft must also supply auxiliary power typically required by narrow-body aircraft, such as the Boeing 737 or Airbus A320. This auxiliary power includes hot bleed air extracted from higher compressor stages of the engine for wing de-icing and other aircraft systems. A literature review estimates this auxiliary power requirement at about 893 kW (1,200 hp) per engine. When sizing a turboshaft engine for DiscThruster operation, these auxiliary power demands must be added on top of basic engine output. Auxiliary aircraft power requirements (e.g., intermittent wing de-icing) are not included in calculating DiscThruster thrust specific fuel consumption (TSFC) as is normally done in industry.

B. Reduction Gearboxes - Large turboshaft engines typically incorporate an integral reduction gearbox within the engine housing to reduce high turbine rotational speed to a more manageable output, typically on the order of 6,000 rpm. A secondary external reduction gearbox is then commonly used to further reduce rotational speed for applications such as a propeller drive or helicopter main-rotor rotation. The DiscThruster requires an additional speed reduction of approximately 3:1 to 2:1, which would ideally be integrated into the turboshaft's primary reduction gearing. For the purposes of this analysis the secondary reduction gearbox is treated as a standalone efficiency loss. Planetary (epicyclic) gearboxes used in such applications are estimated to have efficiencies in the range of 96–99%, corresponding to losses of approximately 1–4%, or an average efficiency loss of 3% assumed for this study (see Ref. 6).

C. Gas Collection and Recompression - The gas component of the two-phase fluid exiting the converging-only rocket nozzles rapidly expands toward atmospheric pressure. Most of this gas is captured by an open-faced, ten-blade impeller (C), which also functions as a gas–liquid separation device. Any remaining gas not intercepted by the impeller is drawn upward by a sidewall axial compressor integrated into the inner wall of the DiscThruster (not shown), assisted by the vortex-induced swirl generated by the rotating impeller. If required, an additional rotating gas-collection stage (not shown), potentially incorporating non-combustion inert gas injection or controlled gas burn-off, may be installed near the DiscThruster exit to capture and manage residual heated gas trying to escape the system. All collected gas is subsequently recompressed by the axial gas compressor and returned to the pressurized side of the system. Assuming a compression ratio of 3:1 for an ideal gas and applying a compressibility correction factor (see Ref. 7), compressor efficiency is estimated to be approximately 95%.

D. Stationary Disc with Integrated Rocket Nozzles - The DiscThruster disc is stationary, incorporating multiple round and/or elongated converging only rocket nozzles in a single nozzle dense concentric circle beneath the path of the rotating ten-blade impeller. During maximum thrust operation (e.g., aircraft takeoff), all rocket nozzles

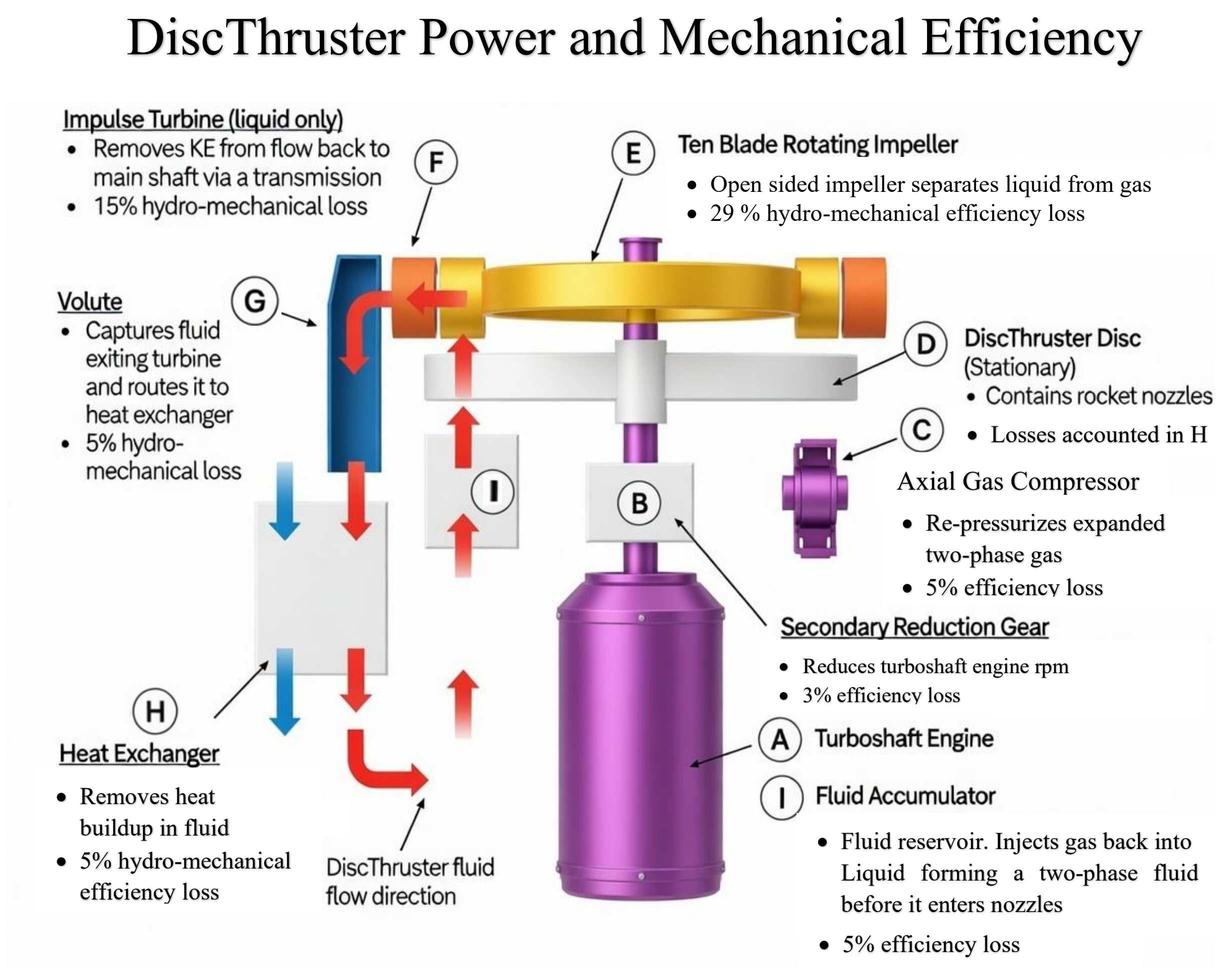

DiscThruster Total Mechanical Efficiency Estimate (η) = 48%

Figure 16   DiscThruster total mechanical efficiency estimate (η) equals 48%.

operate. For reduced-thrust conditions (e.g., climb, cruise or landing), a movable shutter (not shown) selectively blocks a portion of the rocket nozzles to modulate thrust.

In one embodiment (not shown), the DiscThruster disc rotates slowly about its centerline. This rotation imparts tangential velocity to the fluid exiting the rocket nozzles, aiding downstream fluid collection and reducing impeller view-factor blockage of the rocket nozzle exits. The rotational speed is sufficiently low to avoid increasing effective sonic velocity or flow separation within the nozzles due to centripetal acceleration. Losses associated with nozzle wall shear viscous friction, boundary-layer growth, turbulence, and entrance contraction effects are combined with losses attributed to the fluid accumulator (I). In the absence of a high-fidelity design, these losses are represented by a 5% engineering "placeholder" estimate.

E. Rotating Impeller - The primary function of the rotating ten-blade impeller (blade count is not necessarily the optimized value) is to collect two-phase working fluid exiting the DiscThruster disc rocket nozzles, separate the liquid and gas phases, and direct each phase to its appropriate downstream collection point. The open-sided impeller design enables gas–liquid separation under high centripetal loads, directs the high-velocity liquid to the impulse turbine (F) and the gas to the axial gas compressor (C).

The open impeller geometry ensures that the outer radius of the impeller contains only liquid, with no entrained gas, which would otherwise degrade impeller and impulse turbine performance. The sweeping impeller blades partially "shadow" the rocket-nozzle exits; this blocked area must be accounted for when determining the effective total nozzle flow area. A single-stage optimized semi-open radial impeller typically achieves efficiencies in the range of 68–74%, with an average value of approximately 71% (see Ref. 8). The use of a high-density working fluid, such as a bismuth–tin eutectic, may further reduce impeller efficiency.

In one alternate embodiment, the rotating impeller blade's open channel is swept backwards from the direction of rotation, allowing fluid in the channel to accelerate and then exit at its maximum radius tip in the *opposite* direction of blade rotation. By superposition the backward exiting fluid cancels much of the forward speed imparted on the fluid by the rotating impeller blade. It is important to note that a closed channel or tube may not allow the fluid to accelerate as fast as in an open channel if there is back pressure on the closed tube's fluid column. By adjusting the backward fluid exiting angle (e.g., 15° measured from the tangent line where the fluid exits) and radius tip length—you greatly reduce exiting fluid velocity and its kinetic energy. Reducing kinetic energy in the exiting fluid may no longer require an impulse turbine to extract large magnitudes of kinetic energy from the now greatly reduced velocity flow.

DiscThruster Mechanical Efficiency Calculations				
DiscThruster		Component Mechanical Efficiency (η)		
Letter	Component	η (%)	% Loss	Notes
A	Turboshaft Engine	100	0.0	100% shaft output
B	Secondary Reduction Gear	97	3.0	Ref. 6
C	Axial Gas Compressor	95	5.0	Ref. 7
D	DiscThruster Disc (stationary)	Included in I	-	See I.
E	10-Blade Rotating Impeller	71	29.0	Ref. 8
F	Impulse Turbine (liquid only)	85	15.0	Literature Search
G	Volute	95	5.0	Engineering est.
H	Heat Exchanger	95	5.0	Engineering est.
I	Fluid Accumulator	95	5.0	Engineering est.
System Efficiency η (%) =		48		

Table 4 DiscThruster mechanical efficiency estimate (η) equals 48%.

This alternate embodiment still requires a means of directing flow leaving the impeller blade and directing it to the stationary rocket nozzles under high pressure and at a controlled mass flow rate, with unknown losses along the way. For this reason alone, we maintain an impulse turbine in our baseline paper study, and it's better understood (more quantifiable) mechanical efficiency.

F. Impulse Turbine - The impulse turbine is similar in configuration to the design shown in Figs. 11–13. The turbine receives predominantly liquid flow, with little to no entrained gas, from the rotating ten-blade impeller. The incoming fluid velocity is a combination of the nozzle exit velocity and tangential tip velocity imparted by the impeller. The outer radial section of the rotating impeller may incorporate backward-swept blade channels to reduce tangential fluid velocity prior to entry into the impulse turbine.

The turbine reduces fluid velocity by directing it through a 150-170° angle U-like shaped turn passages that extract kinetic energy from the liquid. Recovered kinetic energy is mechanically transferred to the rotating impeller through a geared transmission (not shown), as demonstrated in the most recent DiscThruster working prototype. The rotational speed ratio between the turbine and the impeller is selected to maximize kinetic energy recovery while maintaining sufficient turbine exit velocity to allow recirculation of the liquid back to the DiscThruster disc nozzles with the goal of not increasing or decreasing bulk liquid moving velocity. Higher impulse turbine fluid exit velocities can recover fluid and friction losses along the way to the stationary rocket nozzles and/or to repressurize fluid flow pressure by semi-stagnation flow pressure recovery.

G. Volute - The volute is a toroidal (doughnut-shaped) cavity that receives liquid exiting the impulse turbine with planned residual velocity (see Fig. 16 label G above). This velocity induces a swirling flow pattern within the volute as the fluid travels along the outer-diameter walls. In the absence of a high-fidelity volute design, efficiency losses are difficult to quantify; therefore, a 5% engineering "placeholder" mechanical efficiency loss is assumed for performance loss calculations.

H. Heat Exchanger - The heat exchanger consists of a high-temperature side and a low-temperature side. Liquid exiting the volute enters the high-temperature side and is cooled by fluid heat transfer energy passing within the low-temperature side. The low-temperature side is coupled to a secondary external heat exchanger (not shown), where thermal energy is transferred to cooler ambient air surrounding the aircraft. The primary function of the heat exchanger is to remove excess thermal waste energy generated by mechanical losses as the working fluid circulates through the DiscThruster system. In the absence of a detailed design, a 5% engineering "placeholder" efficiency loss is assumed.

I. Fluid Accumulator - Cooled liquid leaving the low-temperature side of the heat exchanger is directed at the fluid accumulator which serves as temporary fluid conditioning and consolidation reservoir. High-pressure gas from the axial gas compressor (C) is injected into the accumulator to form the desired two-phase working fluid just before it enters the rocket nozzles. Different gas injection methods could be used to potentially reduce the slip ratio (S). Within the accumulator, key fluid properties are adjusted that include velocity, pressure, temperature, and liquid-to-gas volumetric ratio.

J. Risk Assessment and Mitigation (Abatement)

Table 5 presents a 5 × 5 risk-assessment and mitigation (sometimes called a risk-abatement matrix) matrix for the DiscThruster concept. Six major risks are identified, each showing an initial risk level (located at the top of the blue arrow) and a proposed mitigation strategy that aims to reduce the risk to the green "Low Risk" category (located at the bottom of the arrow). Each risk and its corresponding mitigation approach are described in detail below.

This 5 × 5 matrix is not intended to be exhaustive. Additional significant risks are not listed, and many new ones will be discovered as the DiscThruster progresses along the engineering development path.

Six primary RISKS are identified in Table 5 as follows:

1. Sonic Velocity Prediction Uncertainty - Wood's homogeneous equilibrium model (HEM) equation (Eq. 3) may under-predict sonic velocities for two-phase liquid-metal and low gas-volume-fraction mixtures. The slip ratio is not well understood for the baseline condition and may greatly increase sonic velocity substantially. Higher than predicted sonic velocities would directly erode DiscThruster performance.
2. Incomplete Gas Recovery - Inefficient capture of the gaseous component of the two-phase working fluid may allow gas to escape the DiscThruster thrusting cavity, reducing overall system efficiency and performance.
3. High-Temperature Liquid Metal Challenges - Unknown challenges associated with high-temperature liquid metal include handling, flow behavior, potential efficiency degradation (required surface slag oxidation removal), and thermal storage.

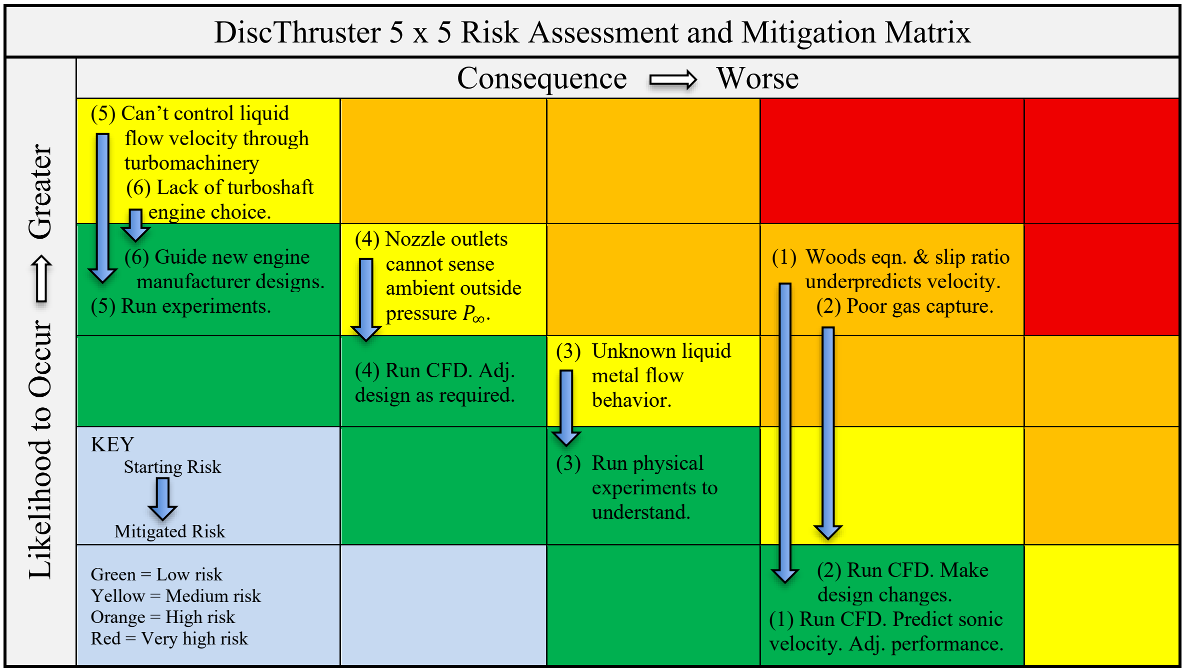

DiscThruster 5 x 5 Risk Assessment and Mitigation Matrix

Consequence ⟹ Worse

Likelihood to Occur ⇧ Greater

🟨 (5) Can't control liquid flow velocity through turbomachinery (6) Lack of turboshaft engine choice.	🟧	🟧	🟥	🟥
🟩 (6) Guide new engine manufacturer designs. (5) Run experiments.	🟨 (4) Nozzle outlets cannot sense ambient outside pressure P_∞.	🟧	🟧 (1) Woods eqn. & slip ratio underpredicts velocity. (2) Poor gas capture.	🟥
🟩	🟩 (4) Run CFD. Adj. design as required.	🟨 (3) Unknown liquid metal flow behavior.	🟧	🟧
KEY Starting Risk ⇩ Mitigated Risk	🟩	🟩 (3) Run physical experiments to understand.	🟨	🟧
Green = Low risk Yellow = Medium risk Orange = High risk Red = Very high risk	🟦	🟩	🟩 (2) Run CFD. Make design changes. (1) Run CFD. Predict sonic velocity. Adj. performance.	🟨

Table 5. Risk matrix identifies major risks and mitigation strategy to reduce all risks to an acceptable level.

4. Incomplete Pressure Recovery at Nozzle Exit - Fluid exiting the stationary DiscThruster disc rocket nozzles (Fig. 16, item D) may fail to experience the full pressure drop across the choking plane, limiting its ability to sense downstream ambient pressure P_∞ and reduce full achievable pressure-thrust.

5. Flow Velocity Control Through Turbomachinery - Inability to accurately control liquid metal flow velocity through the turbomachinery components (e.g., impeller, impulse turbine, heat exchanger) may result in improper inlet conditions at the fluid accumulator (Fig. 16, item I), preventing optimal entry into the DiscThruster rocket nozzles.

6. Turboshaft Engine Availability and Required Production Scale - The baseline DiscThruster thrust requirement of 129 kN (29,000 lbf) necessitates 3.7–5.5+ MW (5,000–7,500+ hp) class turboshaft engines. Only a limited number of legacy or refreshed/advanced legacy engines with acceptable specific fuel consumption (SFC) are currently available and at limited production capacity. These engines are primarily designed for helicopter and tilt-rotor applications that operate in harsh environments, resulting in shorter time between overhaul compared to modern turbofan engines. Furthermore, they are not optimized for Mach 0.78 cruise at altitude, leading to non-optimal SFC when operated under these commercial aircraft flying conditions.

Top six risk MITIGATION strategies identified in Table 5 are as follows:

1. Generate High-fidelity CFD Model for More Accurate Sonic Velocity Prediction - Conduct computational fluid dynamics (CFD) analyses to predict sonic velocities for two-phase liquid metal and low gas volume-fraction mixtures flowing through converging only rocket nozzles. Use supplemental models and experimentation to understand slip ratio (S). Careful selection of CFD software tools are required because some commercial solvers perform poorly in predicting two-phase sonic choking and slip ratios.

2. Gas Capture Optimization via CFD Design Iteration - Use CFD to quantify gas-capture effectiveness. Redesign thrust cavity as needed to achieve 100% gas recovery goal. The baseline approach employs an open-sided ten-blade rotating impeller (Fig. 16, item B) to separate liquid and gas using high centripetal acceleration, then feeds captured gas directly into an axial gas compressor (Fig. 16, item C). Additional measures include a secondary axial (“squirrel-cage”) compressor integrated into the cavity wall to capture residual gas via induced swirl. Another added option are secondary rotating gas collectors or blowers near the cavity exit plus the controlled introduction of inert or combustible gas as required.

3. Liquid Metal CFD and Experimental Validation - Perform CFD analyses explicitly testing liquid metal two-phase working fluids. Complement simulations with targeted physical experimental testing of high-temperature liquid metal handling, flow behavior, slip ratio with gas, and storage (e.g., insulated or vacuum double wall evacuated vessels). Compare empirical results with CFD predictions and adjust DiscThruster design.

4. Pressure Field Mapping Inside and Outside the Thruster Cavity - Conduct CFD studies to map pressure field distributions both inside and downstream of the DiscThruster cavity. Predict net thrust. Modify geometry as required to ensure proper pressure communication across the nozzle choke plane or accept reduced thrust and efficiency where unavoidable.

5. Liquid Metal Velocity Tracking through Turbomachinery - Use CFD to track liquid metal velocity as it passes through all turbomachinery components and accumulates in the fluid accumulator. Where necessary, flow velocity may be adjusted prior to nozzle entry to achieve proper inlet conditions, recognizing that such corrections will reduce overall efficiency. Explore design embodiment where rotating impeller has backward swept flow channels that greatly reduce exiting fluid velocity’s kinetic energy, to the point of not requiring an impulse turbine.

6. Turboshaft Engine Development and Engagement Strategy - Engage with turboshaft and turbofan engine manufacturers to adapt existing designs to DiscThruster short term. Encourage clean-sheet engine development optimized for steady-state, high-altitude cruise operation. Emphasize the comparatively benign DiscThruster operating environment characterized by steady power output rather than the transient, dusty, and harsh conditions typical of helicopter and tilt-rotor missions to—justify extending time between overhaul intervals to that of modern turbofan “on-wing” maintenance schedules. Promote financial incentives of high production volumes for modern narrow-body turbofan engines. CFM Intl. LEAP turbofan engine deliveries exceeded 1,500 units in 2025.

K. DiscThruster Aircraft and Space Propulsion

Table 6 surveys two turbofan engines and three turboshaft engines relevant to the DiscThruster concept. The turbofan engines are CFM International LEAP-1A and LEAP-1B that power the Airbus A320 and Boeing 737 families respectively. Introduced approximately nine years ago, LEAP engines represent among the best thrust specific fuel consumption (TSFC) performance currently achieved in their thrust class for commercial narrow-body aircraft. TSFC values listed are estimates for the turbofan engine *cruise/intermittent* power settings at *altitude*, generally the largest fuel burn flight segment.

The three turboshaft engines listed in Table 6 fall within the 3,677–5,516 kW (5,000–7,500 hp) power class and represent candidates capable of driving the baseline 129 kN (29,000 lbf) thrust DiscThruster engine. These legacy and refreshed/advanced legacy turboshaft engines are primarily designed for large military helicopters and tilt-rotor aircraft. As such, they are not optimized for sustained Mach 0.78–0.80 cruise at 35,000 ft, the intended operating regime for a DiscThruster equipped commercial aircraft. Nevertheless, these engines as they are, or in some adapted version provide a reasonable baseline for this trade study and could serve effectively in early equipped aircraft.

TSFC/SFC values listed for both the turbofan (TSFC) and turboshaft (SFC) engines are for cruise/intermittent power settings. TSFC values presented in Table 6 should be treated as rough order of magnitude estimates. Estimating SFC for turboshaft engines adapted to DiscThruster is particularly challenging since these engines are not designed for high-altitude, high-Mach cruise operation, even though their thermodynamic core design is fundamentally the same as those of turbofan engines. More accurate SFC estimates require direct engagement with engine manufacturers.

To benchmark a conceptual DiscThruster against modern turbofan and rocket propulsion systems, performance goals were established that demonstrate not marginal improvements but transformative “hyper-performance” gains.

DiscThruster Turboshaft Candidates and Turbofan Engines

Engine Type	Manufacturer	Engine and Thrust or Power Class kN (lbf) [kW (hp)]	Approx. TSFC/SFC$^{(1)}$ g/(kN·s) (lbm/(lbf·hr)) [kg/kW·hr] [(lbm/(hp·hr))]	Status
Turbofan	CFM International	LEAP-1A ~109-156 kN (~24,500–35,000 lbf)	~14.4 g/kN·s (~0.51 lbm/(lbf·hr))	In mass production for commercial aircraft.
Turbofan	CFM International	LEAP-1B ~102-129 (~23,000–29,000)	~14.4-15.0 (~0.51-.053)	In mass production for commercial aircraft.
Turboshaft	Honeywell	T55-GA-714A [~3,677 kW] [(~5,000 hp)]	[~.274-.335 kg/kW·hr] [(~0.450–0.550 lbm/hp·hr)]	In low-rate production for US Chinook Helicopter. Higher power version variants in development.
Turboshaft	Honeywell	HTS7500 [~5,516] [(~7,500)]	[~.256-.274] [(~0.420–0.450)]	In development of the Sikorsky-Boeing Defiant X helicopter.
Turboshaft	General Electric	T408 (GE38-1B) [~5,516] [(~7,500)]	[~0.243-0.256] [(~0.400-0.420)]	In full-rate production for CH-53K King Stallion helicopter.

Note:
(1) Treat all flight cruise/intermittent power setting SFC/TSFC values shown as *rough order magnitude.*

Table 6. Turboshaft engine candidates to power DiscThruster and turbofans in the same thrust power class.

DiscThruster performance goals for this study are as follows:

- A 50% reduction in fuel burn relative to modern air-breathing turbofan engines
- A 2X or two-fold increase in Isp (e.g., from 380 s to 760 s Isp) bench marked against modern rocket engines

Table 7 summarizes primary quantitative results of this study.

The average TSFC of modern turbofan engines, taken as the average of the LEAP-1A and LEAP-1B for cruise at altitude equals 14.59 g/(kN·s) (0.515 lbm/(lbf·hr)). For the DiscThruster concept, the turboshaft engine power required, as determined using Eqn. 5, is 4,645 kW (6,316 hp). Multiplying the average fuel mass flow rate derived from Fig. 6 (average of the three candidate turboshaft engines) of 0.273 kg/(kW·hr) [0.448 lbm/(shp·hr)]) by the baseline horsepower and then divide everything by the thrust of 129 kN (29,000 lbf), yields an effective DiscThruster TSFC of 0.278 g/(kN·s) [0.098 lbm/(lbf·hr)].

Based on these calculations, the conceptual DiscThruster exhibits an 81% reduction in fuel burn relative to modern turbofan engines. To align with the stated performance goals and to conservatively account for both known and unknown uncertainties inherent in a conceptual design, a "performance knockdown factor" was added. Applying a performance knockdown factor of 2.6 to the predicted DiscThruster TSFC equals the 50% fuel-burn reduction target relative to state-of-the-art turbofan propulsion. This conservative adjustment provides margin for modeling uncertainty, scaling effects, and unmodeled losses, while showing the DiscThruster concept meets its stated hyper-performance objectives.

The DiscThruster engine core shown in Figure 16 can be adapted to space launch vehicle missions with the following modifications:

1. Electric Motor Replaces Turboshaft Engine - Because ambient oxygen is unavailable at high altitude and in space, the air-breathing turboshaft engine is replaced by an electric motor that drives the DiscThruster.

DiscThruster Meets Aircraft and Space Propulsion Goals with Significant Margin

	Aircraft Engine TSFC g/(kN·s) (lbm/(lbf·hr))				Rocket Engine Isp N/(kg/s) (lbf/(lbm/s))				
Thrust kN (lbf)	Modern Turbofan[1]	Disc-Thruster[2]	Reduction in Fuel Burn (%)	Performance Knockdown Factor (PKF) to Meet 50% Lower Fuel Burn[3]	Modern Rocket Engine[4]	Steam Turbine Power Revovery[5]	Disc-Thruster[6]	Gain in Isp Factor[7]	PKF to Meet 2X or Doubling of Isp[8]
129 (29,000)	14.59 (0.515)	2.78 (0.098)	81	2.6	380	No	2,251	5.9	3.0
						Yes	2,403	6.3	3.2

Notes:
(1) TSFC is the average of the two turbofan engines shown in Table 6.
(2) TSFC is calculated by first using Table 4 and Equation 4 to determine System Efficiency (η). Next Equation 5 calculates turboshaft power required by the DiscThruster. Multiplying the turboshaft power requirement by Table 6's average SFC value for the three turboshaft engines equals Jet A fuel mass flow rate. Dividing the Jet A mass flow rate by the required DiscThruster thrust equals TSFC.
(3) The large performance knockdown factor artificially increases DiscThruster fuel burn to equal a 50% lower fuel burn than modern turbofan engines.
(4) Isp vacuum performance for Space X Raptor 3 engine.
(5) 'No' = No turbine power recovery while 'Yes' = turbine power extracted from steam used to cool DiscThruster goes back to augment electric motor, reducing its load.
(6) DiscThruster performance estimate before applying performance knockdown factor. See Table 8.
(7) Gain in Isp factor = DiscThruster Isp / Modern Rocket Engine Isp.
(8) Performance knockdown factor = DiscThruster Isp / (2 x Modern Rocket Engine Isp).

Table 7. DiscThruster concept beats 50% lower TSFC goal for aircraft and the 2X or doubling in isp goal for spacecraft performance missions by wide margins.

2. Battery Replaces Jet-A fuel - A rechargeable battery supplies electrical power to the motor as the onboard energy source during ascent, replacing Jet-A fuel and ambient atmospheric oxygen.

3. Open-cycle Water-to-Steam Cooling System - In the absence of ambient air for cooling, the closed cycle heat exchanger is replaced with an open-cycle water-to-steam cooling system. Cooling water (or alternatively ethanol) is introduced to the cold side of the heat exchanger (Figure 16, location H), where it absorbs waste heat from the hot side primarily through latent heat of vaporization by flashing to steam.

The resulting high-pressure steam follows one of two paths:

- No Steam-turbine Power Recovery - Steam is vented overboard during ascent.
- Steam-turbine Power Recovery - Steam is expanded through a steam turbine to return shaft horsepower back to the electric motor, reducing battery power demand and modestly increasing specific impulse.

In both cases, cooling-fluid mass expended during ascent is included in specific impulse calculations, analogous to propellant consumption in conventional rocket engines.

4. Treatment of Battery Mass in Isp calculations - Because battery mass does not physically decrease during operation, battery energy depletion is treated as an equivalent mass expenditure. For example, a 45.4 kg (100 lbm) battery fully discharged over 100 seconds corresponds to an effective mass flow rate of 0.454 kg/s (1 lbm/s) for our specific impulse calculations.

When evaluating payload delivery to orbit, assuming spent batteries are not jettisoned during ascent, the full battery mass is subtracted from delivered payload mass to derive an effective payload mass. Applying simple trajectory analyses that compares modern multistage launch vehicles with a conceptual single-stage-to-orbit (SSTO), the DiscThruster vehicle shows the potential for multiplicative payload fraction gains—even after accounting for battery mass carried to orbit.

In the steam-turbine power recovery configuration, steam exiting the heat exchanger retains substantial work potential. Expansion through a conventional steam turbine extracts mechanical power that is returned to the electric-motor drive shaft. Table 8 baselines a commercially available rechargeable battery (see Ref. 8) with a starting specific energy of 395 Wh/kg (179 Wh/lbm) and a maximum continuous charge/discharge rate of 4C, allowing it to fully discharge in approximately 15 minutes, consistent with ascent to low Earth orbit. After applying system-level knockdowns, including adding an energy margin, balance of battery system mass, and motor inefficiency, the effective system-level specific energy is reduced to 261 Wh/kg (118 Wh/lbm), our basis for Isp calculations.

Calculating DiscThruster Isp for Space Launch Vehicle Applications	
Component	Performance Specs for electric/battery and DiscThruster waste heat cooling system
Battery	• Battery Specific Energy (Ref. 8) 395 Wh/kg (179 Wh/lbm) at 4C discharge rate for this commercial battery. 356 Wh/kg (161 Wh/lbm) with10% added charge margin. 274 Wh/kg (124 Wh/lbm) 30% greater system mass e.g., battery racking, power conditioning unit, cables, etc. 261 Wh/kg (118 Wh/lbm) 95% electric motor efficiency. = 261 Wh/kg (118 Wh/lbm) *baseline* specific energy for Isp calculation. • Battery discharge rate. 4,645 kW (6,316 hp) electric motor output. Mass per second discharge = Electric motor output / battery baseline specific energy. 4.944 kg/s (10.900 lbm/s) = (4,645 kW x 1,000 W/kW) / (261 Wh/kg x 3,600 s/hr).
DiscThruster Cooling	• Fluid – Water. Alternate is ethanol. Open loop cooling. Water circulates and collects DiscThruster waste heat by flashing to steam. Replaces air breathing version that uses ambient air-cooled heat exchanger. • Waste energy (enthalpy) absorbed by fluid is primarily latent heat of vaporization. Starting condition: 105 kJ/kg (45.1 BTU/lbm) liquid water at 25ºC (77ºF). Ending condition: 2,801 kJ/kg (1,204 BTU/lbm) saturated steam at 240℃ (464ºF) and 39.7 bar (576 psi) pressure. Net fluid energy gain equals ~ 2,696 kJ/kg (1,159 BTU/lbm). Energy gain may vary since it depends in part on known exiting steam quality. • Mass Flow Rate to Cool DiscThruster. 4,645 kW (6,316 hp) output x 0.52 mech. eff. loss = 2,415 kW (3,239 hp) waste heat. Waste heat divided by waste heat absorbed by steam = 2,415 kW / 2,696 kJ/(kg·s). = 0.900 kg/s (1.984 lbm/s) of water to cool DiscThruster. Fluid leaves vehicle as steam.
Isp and Mass Flow Rate to Produce 129 kN (29,000 lbf) of Thrust	• Total mass flow rate of cooling steam and battery discharge rate for DiscThruster space launch vehicle to produce129 kN (29,000 lbf) of thrust is as follows: 4.944 kg/s (10.900 lbm/s) battery discharge rate. 0.900 kg/s (1.984 lbm/s) of water to cool DiscThruster. = 5.844 kg/s (12.884 lbm/s) Total mass flow rate. Isp = 2,251 s = thrust / mass flow rate = 129 kN (29,000 lbf) / ((5.844 kg/s (12.884 lbm/s)). This is the Isp listed in Table 7 under "DiscThruster," with "'No' Steam Turbine Power Recovery."

Table 8. DiscThruster powered space launch vehicles require a battery/electric motor combination.

To produce 129 kN (29,000 lbf) of thrust, DiscThruster requires 4,645 kW (6,316 hp) of shaft power, corresponding to an equivalent battery mass flow rate of 4.944 kg/s (10.900 lbm/s) (see Table 8 above). Although battery mass remains constant, this equivalent flow rate is used for Isp accounting.

Table 8 also calculates the cooling-water mass flow rate required to absorb DiscThruster waste heat. Water is selected for its high latent heat of vaporization and environmental friendliness. Cooling water introduced into the heat exchanger at location H in Figure 16, heats and flashes to steam at 240 °C (464 °F) and 39.7 bar (576 psi), a slightly lower temperature and pressure of the operating DiscThruster. Based on waste-heat generation and phase-change enthalpy, the required cooling water mass flow rate is 0.900 kg/s (1.984 lbm/s).

Summing battery equivalent "discharge" mass flow rate and cooling-water mass flow yields a total effective mass flow of 5.844 kg/s (12.844 lbm/s). Dividing thrust by this value results in a specific impulse of 2,258 s, representing a conservative baseline for the DiscThruster space launch vehicle without steam-turbine power recovery.

Table 9 describes using a steam turbine to recover mechanical power from the DiscThruster cooling system and return it to the electric motor via a transmission. This power recovery reduces electric motor demand.

The steam turbine is located at the cold-side exit of the heat exchanger in Figure 16 location H, where high-pressure steam exits at 240 °C (464 °F). The steam is routed directly into the turbine. Based on steam table properties and industry standard turbine efficiency of 85%, the turbine is estimated to deliver approximately 257 kW (345 hp) of mechanical power back to the electric-motor shaft.

From Table 9 calculations, recovered power reduces the required electric-motor rating to 4,338 kW (5,917 hp). The corresponding reduction in effective battery mass flow rate increases specific impulse from 2,251 s to 2,403 s, representing a modest improvement of approximately 6%.

Calculating DiscThruster Isp for Space Launch Vehicle Applications	
Component	Steam Turbine Power Recovery Performance Specs
Isp with Steam Turbine Power Recovery	• Entry and exit conditions Entry: 2,801 kJ/kg (1,204 BTU/lbm) - Saturated steam at 240°C (464ºF) and 39.7 bar (576 psi) pressure steam turbine entry conditions. See Table 8 heat exchanger exit conditions and assume industry estimate of 85% turbine efficiency. Exit: 100°C and 1.01 bar (sea level pressure). Exits as wet steam with ~0.90 quality. 271 kW (363 hp) turbine mechanical power recovery using steam tables. 257 kW (345 hp) power recovery with 95% efficient transmission that couples turbine shaft to DiscThruster shaft. • Turboshaft resizing and Isp calculation when turbine mechanical power added 4,338 kW (5,917 hp) = 4,645 kW (6,316 hp) [from Table 8] - 257 kW (345 hp). Isp = 2,403 s = thrust / mass flow rate = 29,000 lbf / (12.884 lbm/s x (5,917 hp / 6,316 hp)). This Isp is listed in Table 7 under "DiscThruster," with "'Yes' Steam Turbine Power Recovery.").

Table 9. Recovering waste heat with a steam turbine modestly boosts Isp 6% to 2,403 s.

L. Applying DiscThruster to Aircraft and Space Applications and the Art of the Possible

DiscThruster applied to commercial aircraft will reduce operating costs since jet fuel is the single largest operating expense. DiscThruster is adaptable and scalable to most commercial aircraft and other applications. For example, a Boeing 737 would retrofit DiscThruster directly to the current aircraft's pylon attach point on the underside of the aircraft by adjusting the vertical length of the pylon to match up to the same thrust vector and alignment position of the previous engine to speed certification. Figure 17 shows a hypothetical installation of DiscThruster on a Boeing 737 aircraft. Turboshaft engine and heat exchanger inlet/outlets are omitted for simplification. Figure 18 shows comparative size between DiscThruster and a turbofan engine.

DiscThruster applied to space launch vehicles has many opportunities as follows:

(1) Single Stage to Orbit (SSTO) One-way Payload Launch - By way of example, if you developed a one-way payload to orbit around 2 x 129 kN (29,000 lbf) thrust engines with steam power recovery, each spinning their electric motors in different directions to cancel any torque issues, and launch time to orbit was set arbitrarily at 12 minutes; the consumable mass of two DiscThruster engines would be:

- Battery Mass – 8,030 kg (17,704 lbm) with 10% built in added contingency
- Cooling Fluid – 1,214 kg (2,676 lbm)

Total consumable mass equals 9,244 kg (20,380 lbm) representing only about 35% of the DiscThruster's gross

Figure 17 Conceptual DiscThruster mounted on a Boeing 737 wing.

Figure 18 Engine size comparison between DiscThruster and turbofan engine where both produce 129 kN (29,000 lbf) thrust.

thrust, understanding you carry the entire battery mass to orbit which subtracts directly from the payload. Still, simplified orbital analysis point to significant gains in payload fraction over conventional launch vehicles.

The SSTO's propulsion section might look like a stubby cylinder about 3 m (9.8 ft) in diameter and 1.5 m (4.9 ft) tall, with battery pack and cooling fluid tanks comfortably nestled inside. Sitting on top of the propulsion section would be a large payload fairing that probably drives the propulsion section's cylinder diameter and payload attach points. At the bottom of the propulsion section would be two protruding DiscThruster engines and landing legs with aerodynamic surfaces attached to them (just an idea not necessarily the baseline design). When ascending the legs point down. When descending they would rotate 180º up to help manage center-of-mass vs. center-of-pressure aerodynamic stability.

(2) SSTO Round-trip Payload Launch - The round-trip version operates similarly to the previous example with the addition of deployable solar cells and extra engine cooling fluid (water or ethanol) for the return trip back to

Earth. Once in orbit the SSTO would deploy moderate sized roll-out-roll-in solar panels to recharge the batteries over about two weeks in orbit. Once the battery was fully recharged the vehicle would perform a controlled power descent and pad landing back on Earth. During descent DiscThruster engines would operate continuously, essentially performing a long deorbit burn and powered vertical descent, never exceeding about Mach 1.5 in the atmosphere, within the maximum continuous operating temperature of commercial bismaleimide-carbon fiber composite structures, avoiding the need for any thermal protection system that would otherwise; add significant mass, eat up payload fraction, create inherent risks including potential burn-through leading to catastrophic vehicle loss, and high maintenance costs. Absence of a thermal protection system promotes rapid vehicle turnaround and lower operating costs.

(3) Endo/Exoatmosphere Operating Commercial Aircraft - Operating in a manner like the previously discussed single-stage-to-orbit (SSTO) round-trip launch vehicle, less solar recharging in orbit (see Figures 19 and 20 updated illustration excerpts from Ref. 3), the proposed Endo/Exoatmosphere commercial aircraft would be capable of transporting 180 passengers (nine wide seating) over intercontinental distances in unprecedented short flight times. Figure 19 depicts basic vehicle configuration and illustrates its relative size compared to a Boeing 737 MAX 9 aircraft. This "art-of-the-possible" concept vehicle would have an estimated gross launch mass of 106,594 kg (235,000 lbm), powered by multiple DiscThruster engines that produce a thrust of 1,570 kN (353,000 lbf), for about a one-hour flight duration.

Figures 19 and 20 show primary operational flight modes. The vehicle takes off vertically with its four small wings tucked below, ascending nearly vertical through the densest layers of the atmosphere, and then transition to forward flight. Forward velocity would increase at high altitude near the interface between atmosphere and space vacuum at the Kármán line at 100 km (62 mi). At this altitude the vehicle is moderately tilted forward to gain speed but maintain altitude. When the vehicle reaches 3,200-3,657+ m/s (10,500-12,000+ ft/s) forward velocity, depending on trip length, it levels out, and thrusts only vertically downward as it coasts in the vacuum of space.

Descent largely mirrors ascent in reverse, with the added capability to loiter in the upper atmosphere using four compact wings for lift. The vehicle descends as an unpowered, low lift-to-drag ratio glider comparable to a sport gliders club's worst glider—hence the "stubby," wide-body fuselage and undersized wing appearance, reflecting the limited fraction of mission time spent in the atmosphere. This configuration enables the vehicle to glide down, essentially "holding" at high altitude with little to no thrust expenditure, allowing it to await clearance from air traffic control before resuming further descent and executing a final vertical landing at the destination airport. Vertical landing eliminates the need for a conventional runway, just a moderate sized round concrete pad.

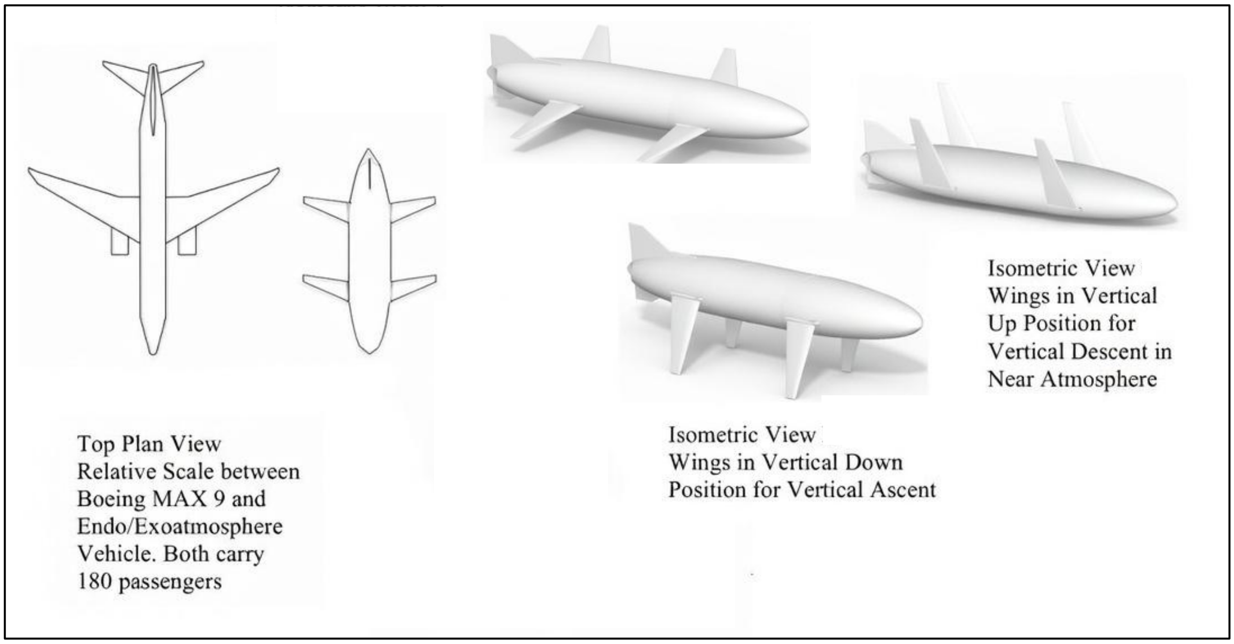

Figure 19 Endo/Exoatmosphere concept aircraft has a wide body and stubby wings since little of its flight time is spent in the atmosphere.

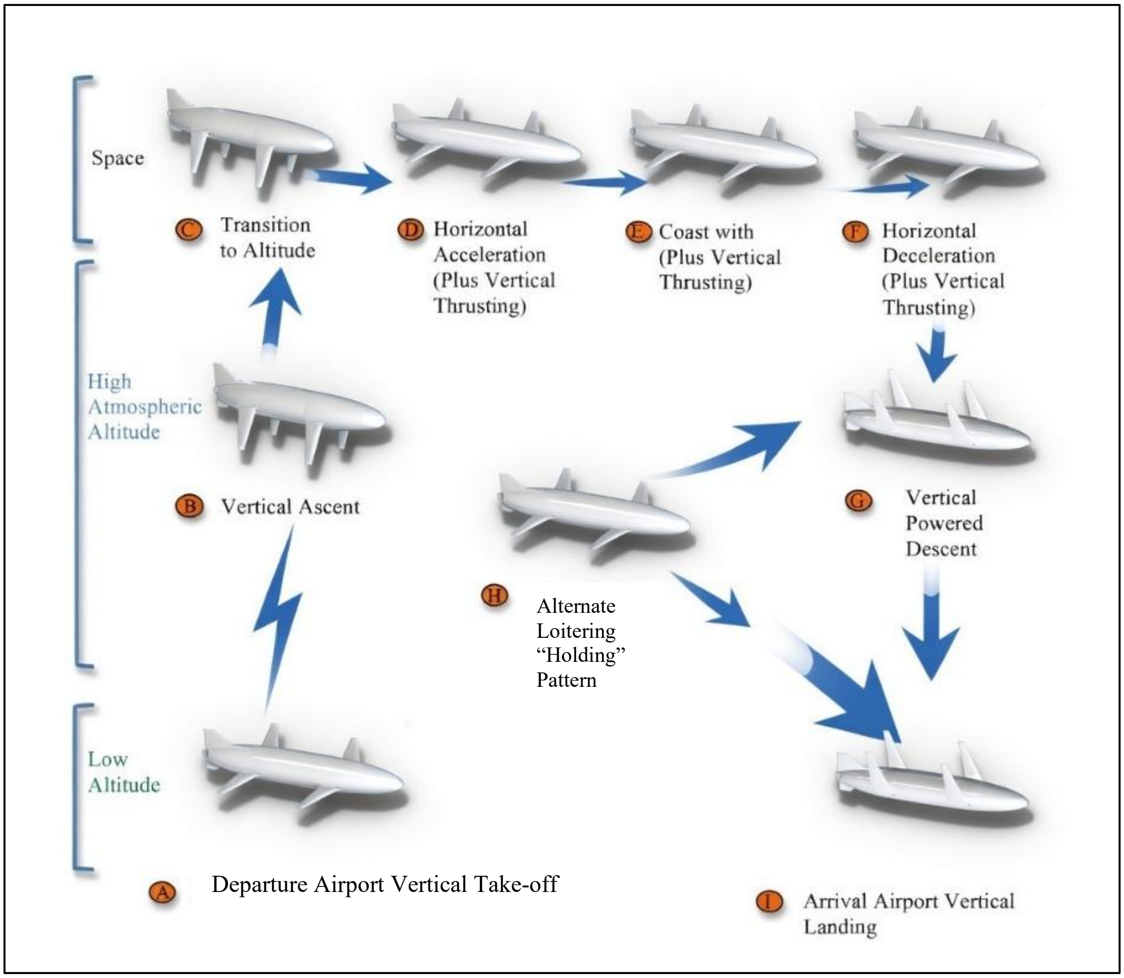

Figure 20 Endo/Exoatmosphere aircraft operational flight modes.

This conceptual endo/exoatmosphere commercial aircraft represents the "art of the possible." With certainty the DiscThruster baseline performance presented in this paper does not come near to meeting specific impulse requirements necessary to enable such mission profile. Breakthrough advances in both propulsion efficiency and battery energy storage are required to realize this vision. But such visions will drive everything else.

IV. Results and Conclusions

Historically, propulsion research has emphasized maximizing momentum-thrust while minimizing pressure-thrust in pursuit of maximum engine performance. The DiscThruster concept fundamentally reverses this paradigm by prioritizing pressure-thrust, enabling the possibility of conceptually *hyper efficient* air breathing and rocket propulsion systems. These potential performance gains arise by avoiding the substantial kinetic energy losses and unrealized work potential associated with the *exiting* high velocity exhaust streams leaving turbofan engines and rocket engines. Instead, DiscThruster focuses on the pressure-thrust component of the rocket equation rather than momentum-thrust.

Initial investigations began with a simple thrust stand in which a two-phase fluid consisting of water and air was driven through a converging-only rocket nozzle and sonically choked at the throat at relatively *low* flow velocities. Low flow velocities equal low kinetic energy losses leaving the system. Building on these early experiments, the first DiscThruster prototype, a 24 cm (9.5 in) diameter disc fabricated using 3-D printed plastic and overwrapped with Kevlar fiber, was successfully operated at rotational speeds up to 5,300 rpm. This rotating disc demonstrated that centripetal forces could pressurize and drive fluid through multiple rocket nozzles while simultaneously bending the flow through a 90° turn, an essential precursor to fluid capture and recycling in subsequent configurations.

The next design iteration incorporated lessons learned from earlier prototypes and introduced two key features: (1) an impulse turbine to recover kinetic energy from high-velocity fluid flow, and (2) a toroidal (doughnut-shaped) volute to *capture* and *recycle* fluid back to the DiscThruster. Experiments using this spinning disc yielded promising results, identifying a clear path toward a scalable DiscThruster propulsion system capable of powering both commercial aircraft and space launch vehicles, with *hyper performance* levels exceeding current state-of-the-art.

Table 10 (excerpt from Table 7) summarizes analytical performance results presented in this paper. The DiscThruster concept exceeds, by a wide margin, performance targets corresponding to a 50% reduction in fuel burn over modern turbofan engines and a two-fold (2X) increase in the specific impulse (Isp) over modern rocket engines. These wide margins, reflected in large performance knockdown factors, will be allocated against future uncertainties and unknowns. A good starting place to challenge these hyper performance claims by rigorous *independent* study and testing.

	Aircraft Engine TSFC g/(kN·s) (lbm/(lbf·hr))				Rocket Engine Isp N/(kg/s) (lbf/(lbm/s))				
Thrust kN (lbf)	Modern Turbofan	Disc-Thruster	Reduction in Fuel Burn (%)	Performance Knockdown Factor (PKF) to Meet 50% Lower Fuel Burn	Modern Rocket Engine	Steam Turbine Power Recovery	Disc-Thruster	Gain in Isp Factor	PKF to Meet 2X or doubling of Isp
129 (29,000)	14.59 (0.515)	2.78 (0.098)	81	2.6	380	No	2,251	5.9	3.0
						Yes	2,403	6.3	3.2

Table 10 DiscThruster concept promises hyper performance gains in TSFC and Isp over modern turbofan and rocket engine counterparts with a large starting performance margin for unknowns (see Table 7).

V. References

Paper Publications

1. S.W Kieffer, "Sound speed in liquid-gas mixtures: water-air and water-steam," Journal of Geophysical Research 82(20, 2895-2904 (1977).
2. M. Ishii and T. Hibiki, Thermo-Fluid Dynamics of Two-Phase Flow (2nd Edition) Springer, 2011 (Chapter 7: "Sonic Velocity in Two-Phase Flow," Section 7.3 on homogeneous equilibrium model with slip corrections).
3. Brad Pande, "Disruptive Propulsion Technology Makes Endo/Exoatmosphere Operating Commercial Aircraft Possible, AIAA 2016-4707 Session: Advanced Vehicle Systems Concepts. Published Online: 22 Jul 2016 https://doi.org/10.2514/6.2016-4707.
4. John Bradley Pande, "DiscThruster, pressure thrust based aircraft engine." US Patent application No. US-20160208742-A. Application published date 2016-07-21.

General References

5. Gearbox Design and Efficiency, Planetary Gearboxes (Epicyclic Gearboxes), True Geometry, blog.truegeometry.com.
6. Gas Processors Suppliers Association (GPSA) Engineering Data Book 14th Edition (2020), Section 13 – Compressors.
7. Hydraulic Institute Standards (ANSI/HI 1.3-2012 & 14.6-2016). Performance charts for single-stage centrifugal pumps show open impellers averaging 68–74% at best efficiency point (BEP) for water-like fluids.
8. Amprius Technologies (Amprius.com). 1180 Page Ave, Fremont, CA 94538. Per brochure SiMaxx balanced Lithium-ion silicon-anode platform provides 395 Wh/kg and a 4C continuous discharge rate.

General Disclosure

9. Figures 1, 2, and 17-20 were generated in singular or in combination with Super Grok®, Claude®, and Chat-GPT® artificial intelligence photo visualization software, starting from original author work illustrations and photos.
10. This manuscript of author's original work was written using Microsoft Word® and refined with Microsoft Copilot® using the following instructions: "fix spelling, grammar, and make it sound more professional."
11. DiscThruster is a non-registered trademark of iPropulsion LLC, Midway, UT 84089. DBA iPropulsion.
12. Contact information. Company email: brad.pande@ipropulsion.com or personal email: brad.pande@gmail.com Personal cell: 801.828.0897.